Heavy Quarkonium Production at Hadron Colliders

Kuang-Ta Chao

School of Physics, Peking University

Based on: Phys.Rev.Lett.106,042002(2011), Phys.Rev.D83,111503(2011), Phys.Rev.D84,114001(2011), Phys.Rev.Lett.108,242004(2012), Phys.Rev.D85,114003(2012)

Jefferson Lab

24 August, 2012

Low lying charmonium spectrum (J/ψ, ψ(2S) and χ_cs)

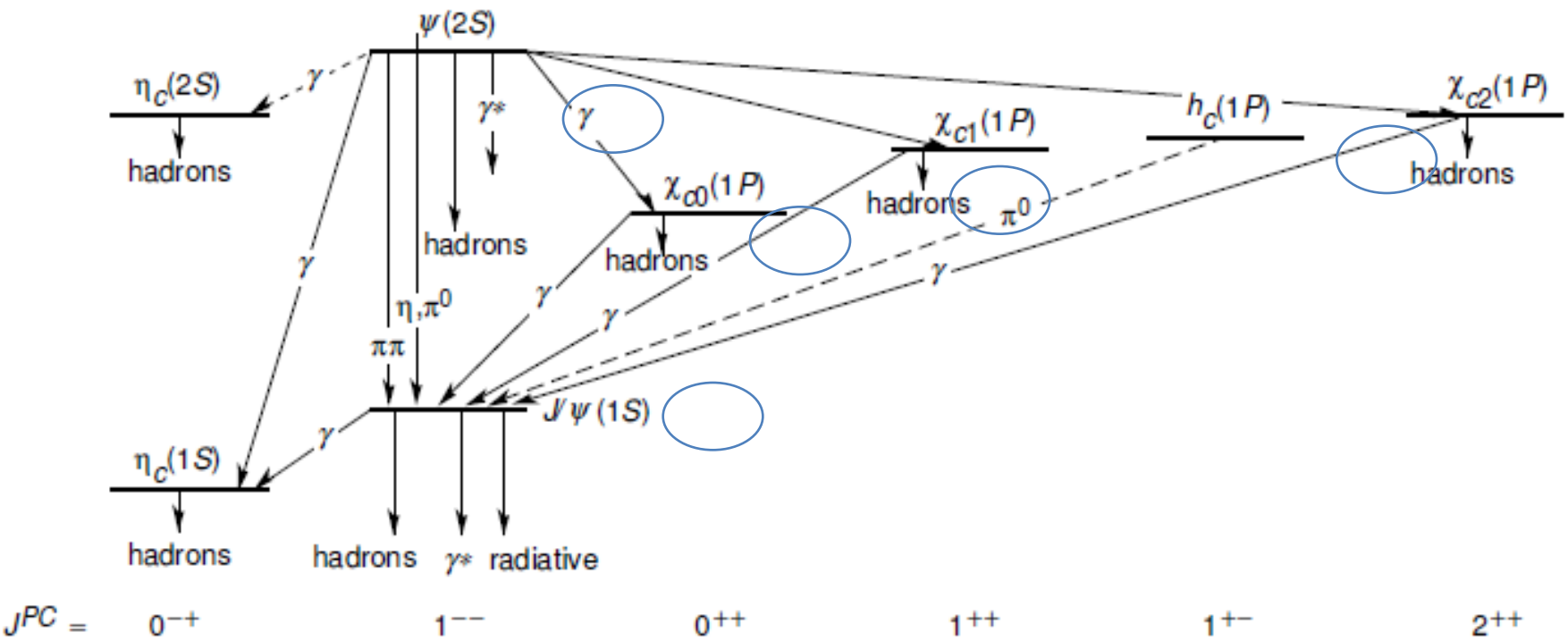

Production in p-p collisions

- Heavy quarkonia are an excellent laboratory for understanding QCD:
  - non-relativistic due to the high mass
  - non-perturbative effects can be simplified and constrained

Color Singlet Model

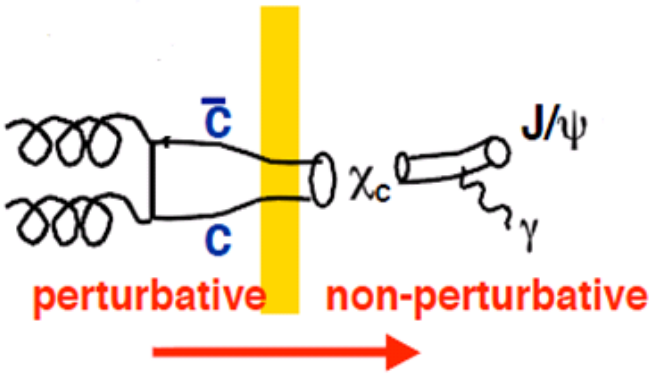

- Long standing puzzles for cross-section and polarization measurements and theoretical calculations, still not satisfactory resolved:
  - cross section results support NRQCD COM
  - polarization not conclusive

Color Octet Model (NRQCD)

Matrix Elements

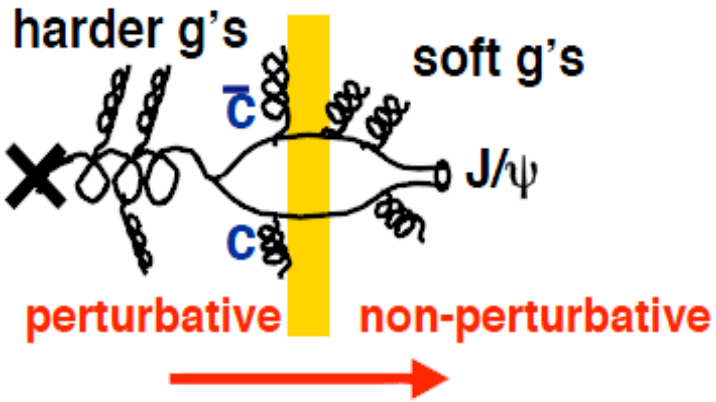

- In the last decade, significant progress for production mechanisms:
  - new experimental results
  - improved theoretical descriptions

LHC and ATLAS, CMS, LHCb

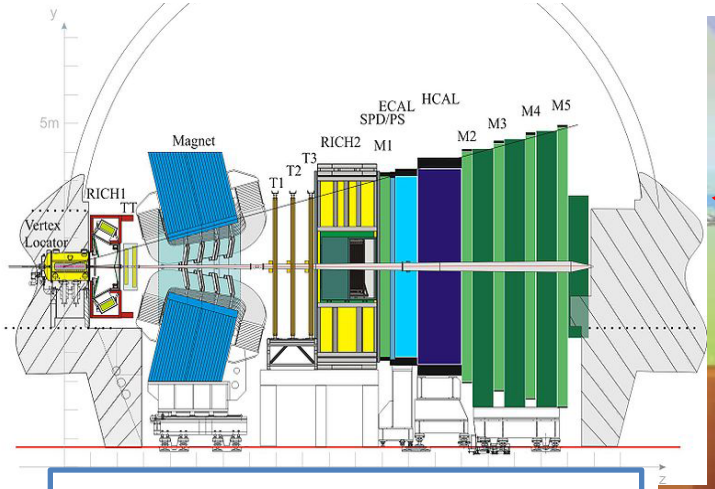

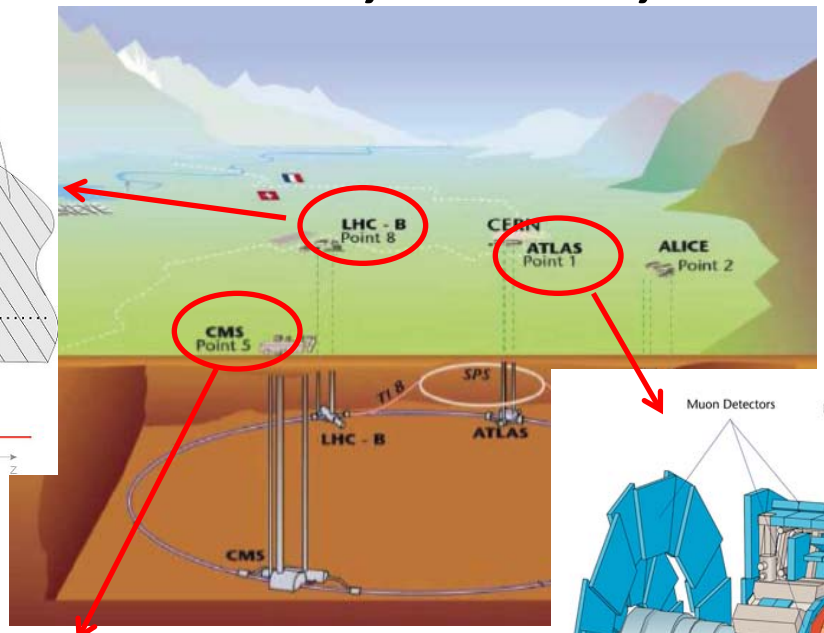

dedicated experiment for Heavy Flavor physics

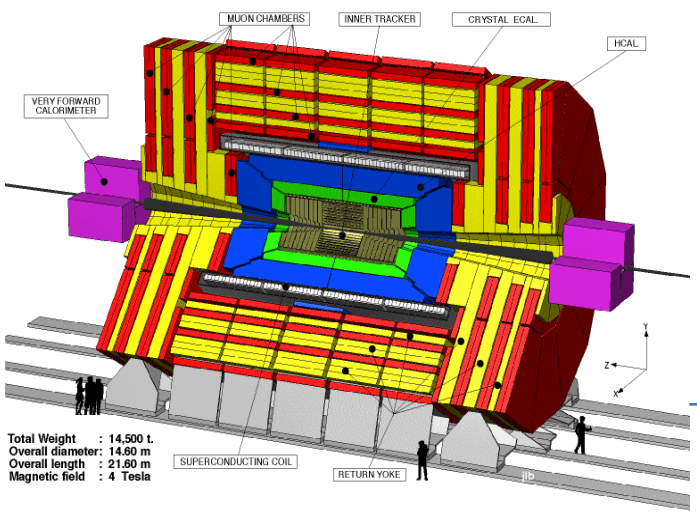

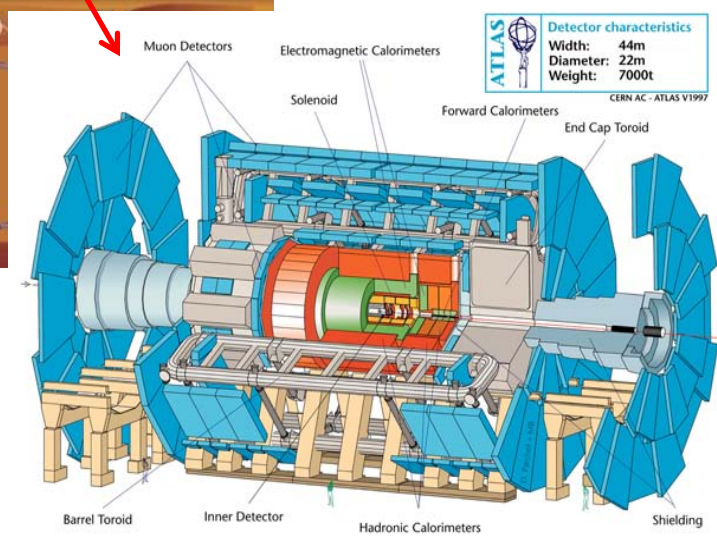

General purpose experiments

Detector Performance

- Muon coverage:
  - ATLAS/CMS: $|\eta| < 2.4$
  - LHCb: $2.0 < \eta < 4.5$

- Detectable quarkonia rapidity and p_T ranges depend on muon acceptance:
  - high p_T only accessible at ATLAS/CMS

mass resolutions (in MeV/c^2):

	$J/\psi \rightarrow \mu\mu$	$\chi_c \rightarrow J/\psi\ \gamma$
LHCb	12	~15 ($\gamma \rightarrow ee$) 18.3 (non-converted)
CMS	20-71	9.6 ($\gamma \rightarrow ee$)
ATLAS	46-111	~36 (ECAL)

	ATLAS/CMS	LHCb
Triggers	Challenging	Not a problem
Resolution	Better for $\gamma \rightarrow ee$ (best in CMS)	Better for dimuons/vertices
p_T-y coverage	$\|y\| < 2.4$, access to very high p_T	Forward rapidity, low p_T

Theoretical and Experimental Issues

- Theoretical framework
- Comparison between theory and experiment
- Improved theoretical results I: yields
  - Why higher-order corrections are important?
  - Predictions v.s. LHC and RHIC data (J/Ψ , Ψ (2S), Υ, χ_c)
- Improved theoretical results II: polarizations
  - Polarizations in the angular distributions
  - J/Ψ polarization at the Tevatron and LHC
  - χ_c polarization at the LHC

Theoretical Framework

Theoretical status

- Large mass scale: pQCD applicable but long standing issues exist in heavy quarkonium production mechanism.
- CSM (see e.g. *M.B.Einhor et al. (1975), C.H.Chang(1980)*): the heavy quark pair is produced in color-singlet states at short distances. P-wave is infrared-unsafe and incapable of interpreting heavy quarkonia production in high-pT region.
- CEM (see e.g. *H.Fritzsch et al. (1977)*): under the assumption of quark-hadron duality, the charm quark pair with its invariant mass between $2m_c$ and $2m_D$ evolves into charmonium. The fixed ratio of $\sigma_{J/\psi} : \sigma_{\chi_{cJ}} : \sigma_{\eta_c} : \ldots$ predicted by it is in contradiction with experimental measurements.
- NRQCD (see e.g. *G.T.Bodwin et al. (1995)*): in addition to the color-singlet intermediate states, there are also color-octet intermediate states produced at short distances. The infrared-divergences in the color-singlet P-wave are cancelled by the CO S-wave long distance matrix elements.

Factorization

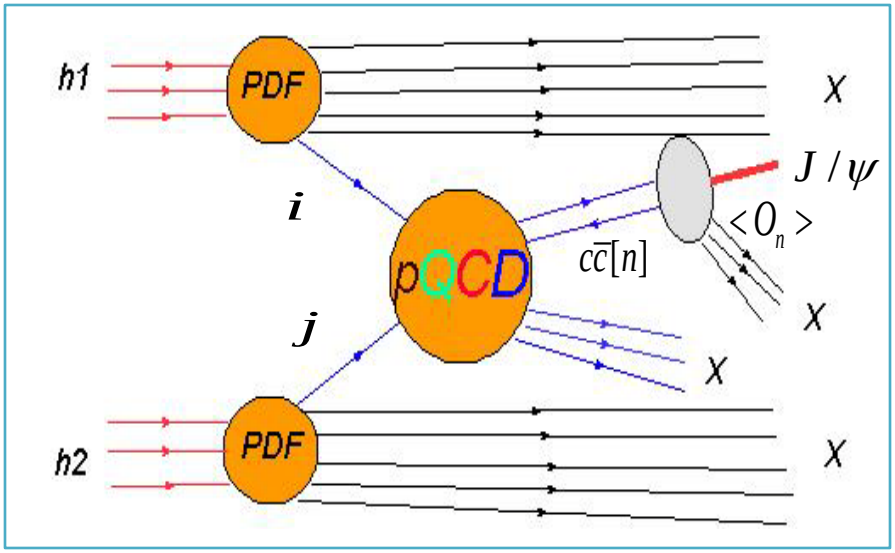

- QCD factorization:

$$\sigma_{hadron} = f_{i/h1} \otimes f_{j/h2} \otimes \sigma^{ij}_{parton}$$

- NRQCD factorization *G. Bodwin et al. (1995)*:

$$\sigma^{ij}_{parton} = \sigma(ij \to c\bar{c}[n] + X) < O_n >$$

- The short distance parton level cross section is perturbative and process-dependent.
- The parton distribution functions and long distance matrix elements $< O_n >$ are non-perturbative but universal.
- The long distance matrix elements are matrix elements of four-fermion operators in NRQCD: $\langle O_n \rangle = \langle 0 | \chi^{\dagger} \kappa_n \psi (\sum_X | H + X \rangle \langle H + X |) \psi \ \kappa_n \chi | 0 \rangle$
- The long distance matrix elements are scaled by v: $v_c^2 \approx 0.23, v_b^2 \approx 0.08$

Fock states expansion in v

k	η_c, η_b	$J/\psi, \psi', \psi(3s)...$ $\Upsilon, \Upsilon(2s), \Upsilon(3s)...$	h_c, h_b	χ_{cJ}, χ_{bJ}
3	${}^1S_0^{(1)}$	${}^3S_1^{(1)}$	—	—
5	—	—	${}^1P_1^{(1)}, {}^1S_0^{(8)}$	${}^3P_J^{(1)}, {}^3S_1^{(8)}$
7	${}^1S_0^{(8)}, {}^3S_1^{(8)}, {}^1P_1^{(8)}$	${}^1S_0^{(8)}, {}^3S_1^{(8)}, {}^3P_J^{(8)}$	—	—

L.Gang et al. (2012)

TABLE I: Values of k in the velocity-scaling rule $\langle \mathcal{O}^{\mathcal{Q}}[n] \rangle \propto v^k$ for the leading $Q\bar{Q}$ Fock states n pertinent to $\mathcal{Q}$.

Challenges in P-wave !

Experiment v.s. Theory

ψ' and J/ψ puzzle

- In 1992, CDF collaboration found a surprisingly large production rate of Ψ' at high p_T.
- As shown on the right Fig, the yield is larger than theoretic predictions by a factor of 30-50, even though the fragmentation contribution is included.

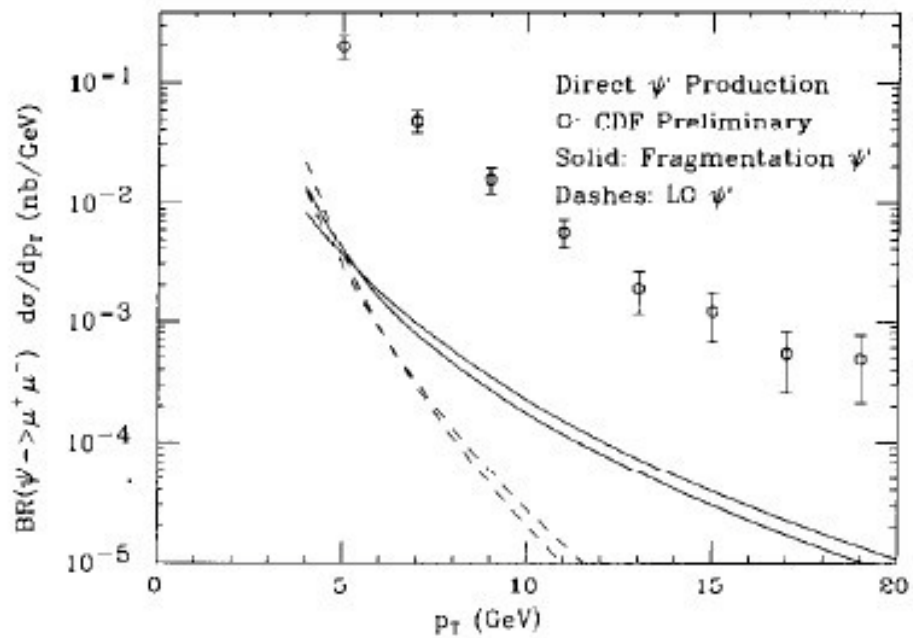

Fig. 4. Preliminary CDF data for prompt ψ' production (O) compared with theoretical predictions of the total fragmentation contribution (solid curves) and the total leading-order contribution (dashed curves).

E. Braaten et al. (1994)

Color-Octet mechanism

States	p_T behavior at LO
$^3S_1^{[1]}$	p_T^{-8}
$^3S_1^{[8]}$	p_T^{-4}
$^1S_0^{[1,8]}$	p_T^{-6}
$^3P_J^{[1,8]}$	p_T^{-6}

- To solve the Ψ' puzzle, the color-octet (CO) mechanism was proposed by Braaten and Fleming based on the NRQCD factorization.
- The CO state contributions decrease much slower compared with the p_T^{-8} of color-singlet (CS) state, and give an natural explanation of the observed experiment data.

E.Braaten, S.Fleming 1996

See a review by M.Kramer, arXiv:hep-ph/0106120

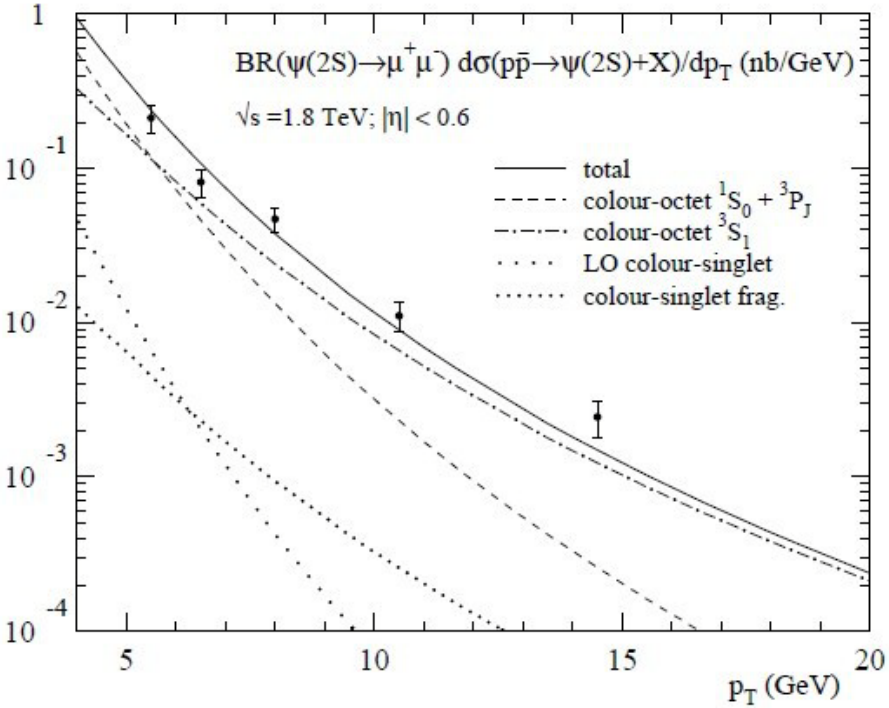

Polarization anomaly

- Although it seems to be able to explain the differential cross sections, CO encounters difficulties when the polarization is taken into consideration.
- Dominated by gluon fragmentation to $^3S_1^{[8]}$ at large p_T, LO NRQCD predicts a sizable transverse polarization (the gluon is almost on shell), while the measurement gives almost unpolarized ψ.
- In gluon fragmentation, the spin-flip interaction is suppressed by v^2(*Cho, Wise (1994)*), and it is verified in a lattice calculation of decay matrix elements(*Bodwin et al. (2005)*).

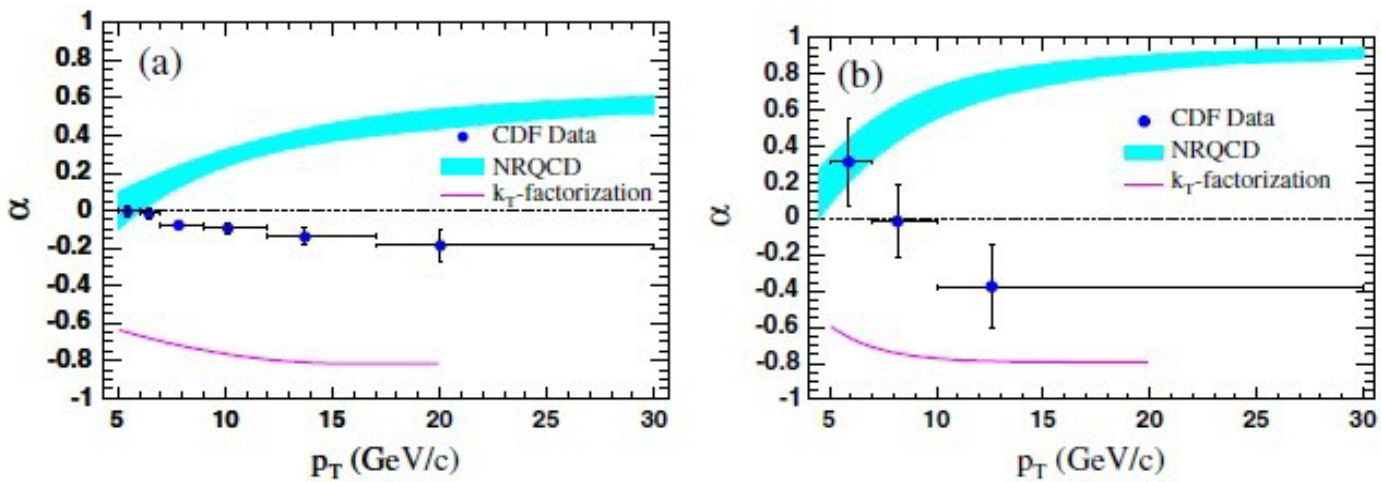

FIG. 4 (color online). Prompt polarizations as functions of p_T: (a) J/ψ and (b) $\psi(2S)$. The band (line) is the prediction from NRQCD [4] (the k_T-factorization model [9]).

A. Abulencia et al. (2007)

χc cross section ratio

$$R \equiv \sigma_{\chi_{c2}} / \sigma_{\chi_{c1}}$$

- CDF (*CDF Collaboration (2007)*) measures R~0.75.
- In NRQCD factorization, the LO χc production is dominated by CO intermediate states at high-pT, which predicts R-> 5/3 by simple spin counting.
- While the LO CSM prediction is much lower than the CDF data.
- The data tell us that one may need a cancelation between CO and CS states.

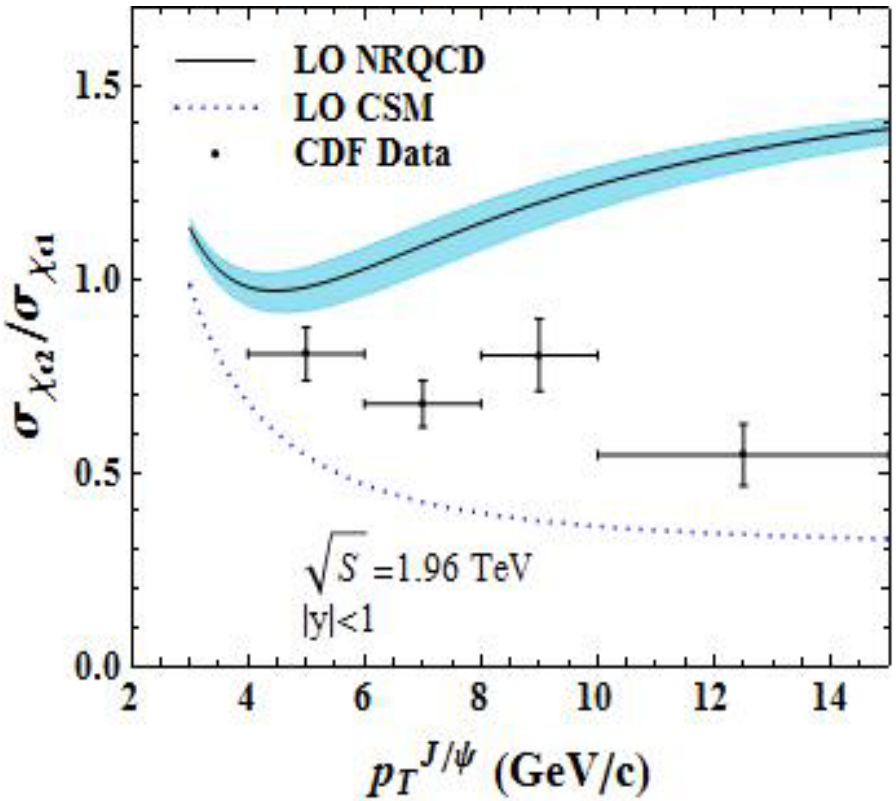

Q1: How to solve these discrepancies ?

Q2: Is NRQCD factorization violated ?

Q3: How about the beyond leading-order results, since the new topology may change the large pT behavior?

Yields

Large k factor

- The NLO color-singlet differential cross section is enhanced by 2 orders relative to LO $^3S_1^{[1]}$ result at high pT.
- On the other hand, the QCD corrections to $^3S_1^{[8]}$ channel is small.

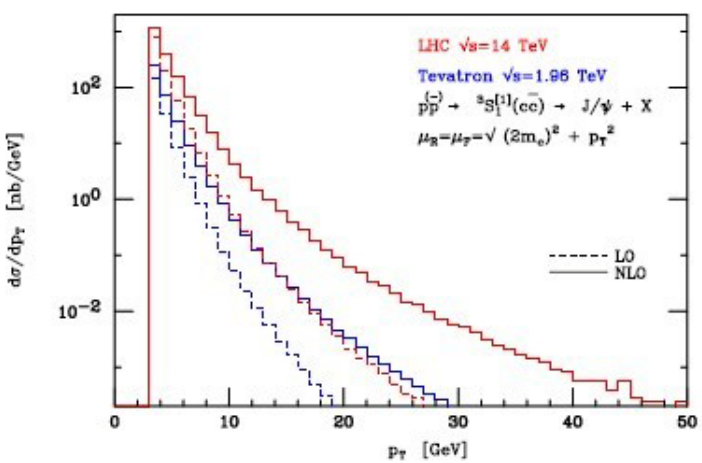

FIG. 5 (color online). Differential cross sections for direct J/ψ production via a $^3S_1^{[1]}$ intermediate state, at the Tevatron (lower histograms) and LHC (upper histograms), at LO (dashed line) and NLO (solid line). $p_T^{J/\psi} > 3$ GeV and $|y^{J/\psi}| < 3$. Details on the input parameters are given in the text.

J.M.Campbell et al. (2007)

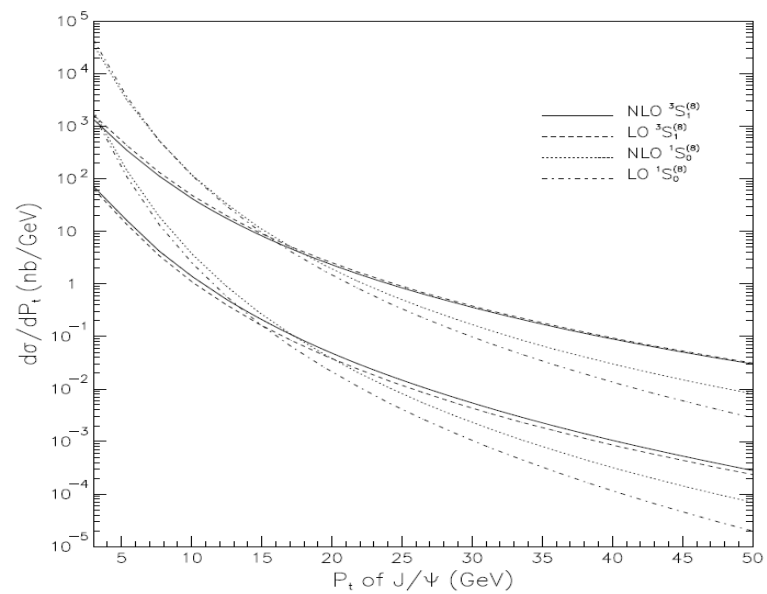

Fig. 3. Transverse momentum distribution of J/ψ production with $\mu_r = \mu_f = \mu_0$ at LHC (upper curves) and Tevatron (lower curves).

B.Gong et al. (2009)

Topological origin

LO color-singlet

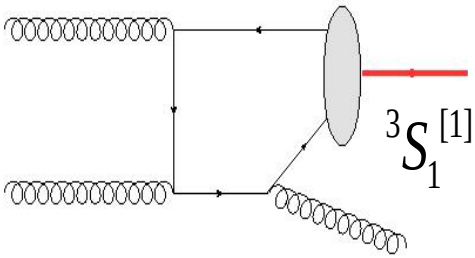

$^3S_1^{[1]}$

$$\sim \alpha_S{}^3 m_H^4 p_T^{-8}$$

LO color-octet

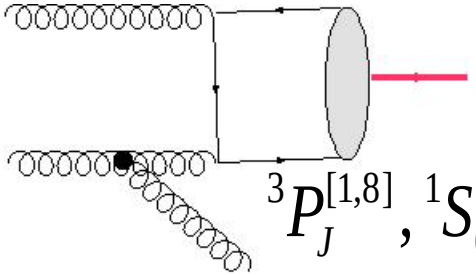

$^3P_J^{[1,8]}, {}^1S_0^{[1,8]}$

$$\sim \alpha_S{}^3 m_H^2 p_T^{-6}$$

LO color-octet

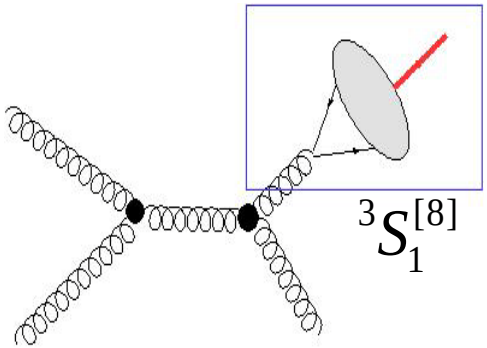

$^3S_1^{[8]}$

$$\sim \alpha_S{}^3 p_T^{-4}$$

States	p_T behavior at LO
$^3S_1^{[1]}$	p_T^{-8}
$^3S_1^{[8]}$	p_T^{-4}
$^1S_0^{[1,8]}$	p_T^{-6}
$^3P_J^{[1,8]}$	p_T^{-6}

Topological origin

NLO color-singlet

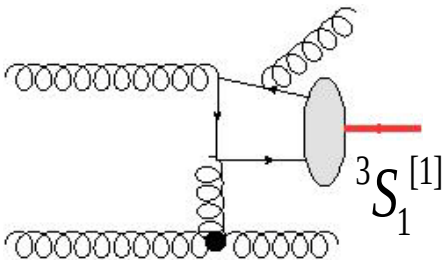

$^3S_1^{[1]}$ $\sim \alpha_S^{\,4} m_H^2 p_T^{-6}$

NLO color-octet

$^3P_J^{[1,8]}, {}^1S_0^{[1,8]}$

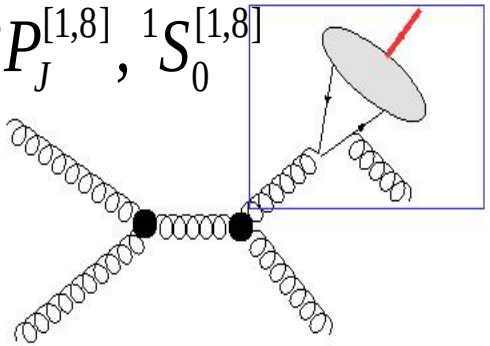

$\sim \alpha_S^{\,4} p_T^{-4}$

NNLO color-singlet

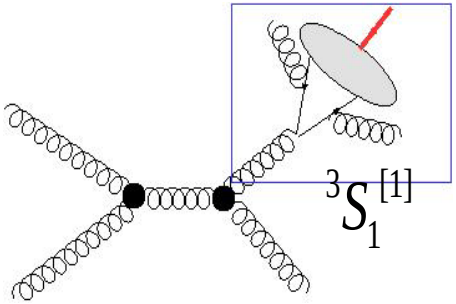

$^3S_1^{[1]}$ $\sim \alpha_S^{\,5} p_T^{-4}$

States	p_T behavior at NLO
$^3S_1^{[1]}$	p_T^{-6}
$^3S_1^{[8]}$	p_T^{-4}
$^1S_0^{[1,8]}$	p_T^{-4}
$^3P_J^{[1,8]}$	p_T^{-4}

CSM

J.P.Lansberg (2011)

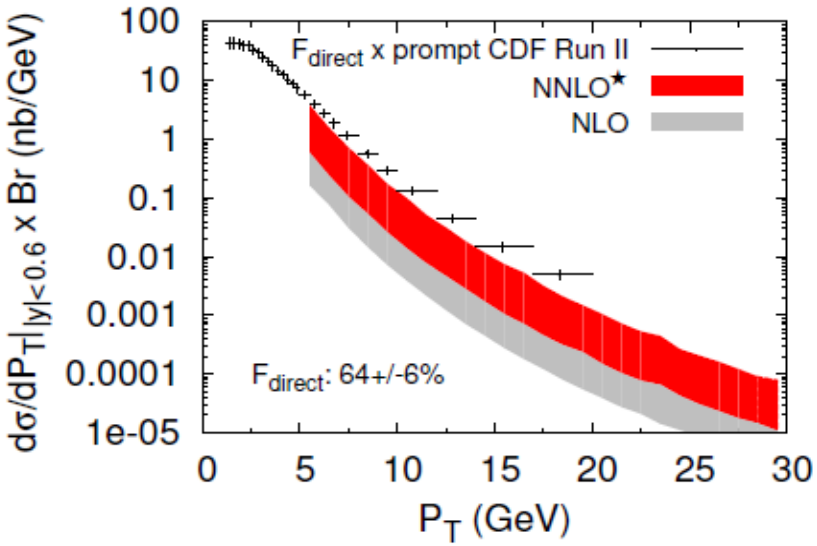

P.Artoisenet et al. (2007)

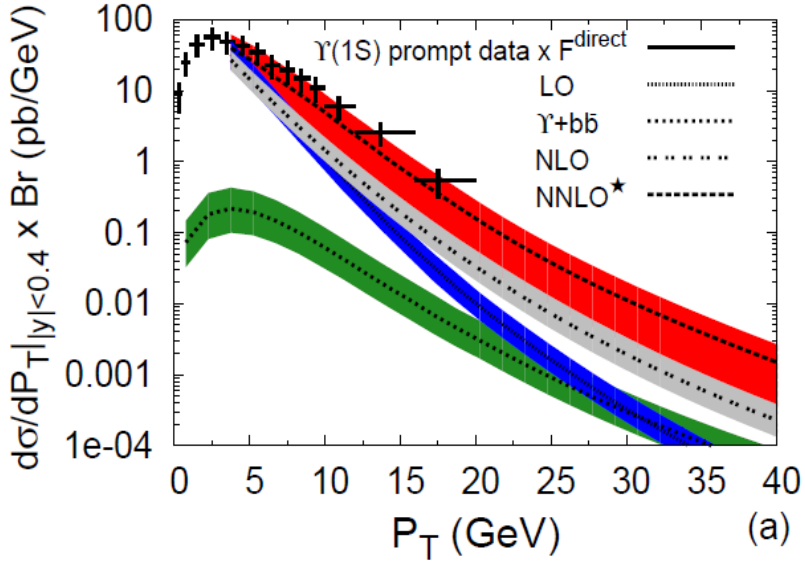

- Even after including NNLO*, the theoretical J/ψ distribution is still below the CDF data, though the situation seems better in Y case.
- *Y.Q.Ma et al. (2011)*: The color-singlet NNLO* corrections at high-pT seem to be dominated by the $\log^2(p_T^2 / p_{Tcut}^2) p_T^{-6}$ term. This term will disappear in the complete NNLO result. Hence the NNLO corrections may not be important.

p_T enhancement is essential

- NLO correction for $^3S_1^{[1]}$ channel implies: kinematic enhancement is very important for heavy quarkonia production at large p_T.
- NLO correction for $^3S_1^{[8]}$ channel is small, because at LO it already contains a non-vanishing p_T^{-4} term and the higher-order correction is suppressed by α_s .
- One cannot draw any definite conclusion until one has reached the order that contains the p_T^{-4} topological diagrams .

States	Order where p_T^{-4} present
$^3S_1^{[1]}$	NNLO
$^3S_1^{[8]}$	LO
$^1S_0^{[1,8]}$	NLO
$^3P_J^{[1,8]}$	NLO

At large pT complete NLO corrections (CS+CO) are essential

- Since NNLO correction to $^3S_1^{[1]}$ channel is out of current state of the art, we may estimate its contribution in the following way:
  - The only new behavior, which scales as p_T^{-4} , is the gluon fragmentation. Other contributions at this order is suppressed by α_s relative to NLO.
  - The fragmentation contribution has been calculated (*E. Braaten et al.1993*), and they are as small as 1/30 of the experimental data for J/Ψ production.
  - So it is possible that we can ignore the NNLO $^3S_1^{[1]}$ contribution safely.

Decomposition of P-wave channel conttributions

Y. Q.Ma, K.Wang, KTC (2010)

- Because of the large k factor of P-wave channel, $^3S_1^{[8]}$ channel is no longer the unique source at high p_T. We find the following decomposition holds within errors of a few percent:

$$d\hat{\sigma}[^3P_J^{[8]}] = r_0\, d\hat{\sigma}[^1S_0^{[8]}] + r_1\, d\hat{\sigma}[^3S_1^{[8]}]$$

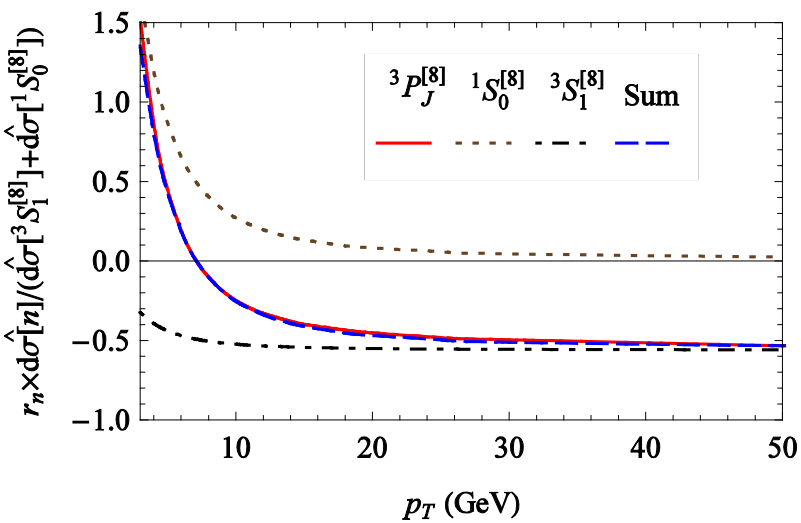

NLO short-distance coefficients of $d\hat{\sigma}[^3P_J^{[8]}]$, $r_0\, d\hat{\sigma}[^1S_0^{[8]}]$, $r_1\, d\hat{\sigma}[^3S_1^{[8]}]$ and Sum=$r_0\, d\hat{\sigma}[^1S_0^{[8]}]$+$r_1\, d\hat{\sigma}[^3S_1^{[8]}]$ in Tevatron.

- As a result, we will use two linearly combined LDMEs:

$$M_{0,r_0}^{J/\psi} = \langle \mathcal{O}^{J/\psi}(^1S_0^{[8]})\rangle + \frac{r_0}{m_c^2}\langle \mathcal{O}^{J/\psi}(^3P_0^{[8]})\rangle$$

$$M_{1,r_1}^{J/\psi} = \langle \mathcal{O}^{J/\psi}(^1S_0^{[8]})\rangle + \frac{r_1}{m_c^2}\langle \mathcal{O}^{J/\psi}(^3P_0^{[8]})\rangle$$

$\sqrt{S}$(TeV)	region of y	r_0	r_1
1.96	(0 ,0.6)	3.9	-0.56
7	(0 ,0.75)	4.0	-0.55
7	(0.75,1.50)	3.9	-0.56
7	(1.50,2.25)	3.9	-0.59
7	(0 ,2.4)	4.1	-0.56
7	(0 ,1.2)	4.1	-0.55
7	(1.2,1.6)	3.9	-0.57
7	(1.6,2.4)	3.9	-0.59
7	(2.5, 4)	3.9	-0.66
7	(2 ,2.5)	4.0	-0.61
7	(2.5, 3)	4.0	-0.65
7	(3 ,3.5)	4.0	-0.68
7	(3.5, 4)	4.0	-0.74
7	(4 ,4.5)	4.2	-0.81
14	(0 , 3)	3.9	-0.57

Fit LDMEs using Tevatron Data

p_T^{cut} GeV	H	$\langle \mathcal{O}^H \rangle$ GeV^3	M^H_{1,r_1} 10^{-2} GeV^3	M^H_{0,r_0} 10^{-2} GeV^3	$\chi^2/d.o.f.$
7	J/ψ	1.16	0.05 ± 0.02	7.4 ± 1.9	0.33
	ψ'	0.76	0.12 ± 0.03	2.0 ± 0.6	0.56
5	J/ψ	1.16	0.16 ± 0.05	5.2 ± 1.3	3.5
	ψ'	0.76	0.17 ± 0.04	1.1 ± 0.3	2.2

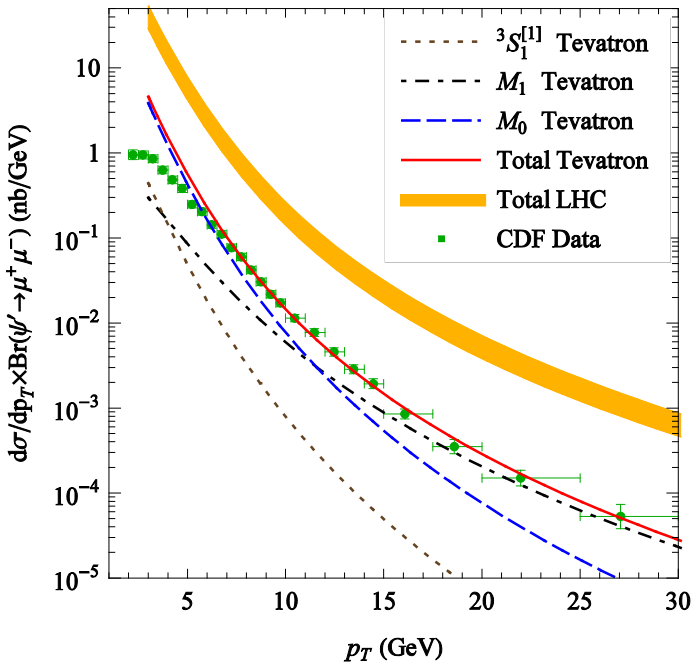

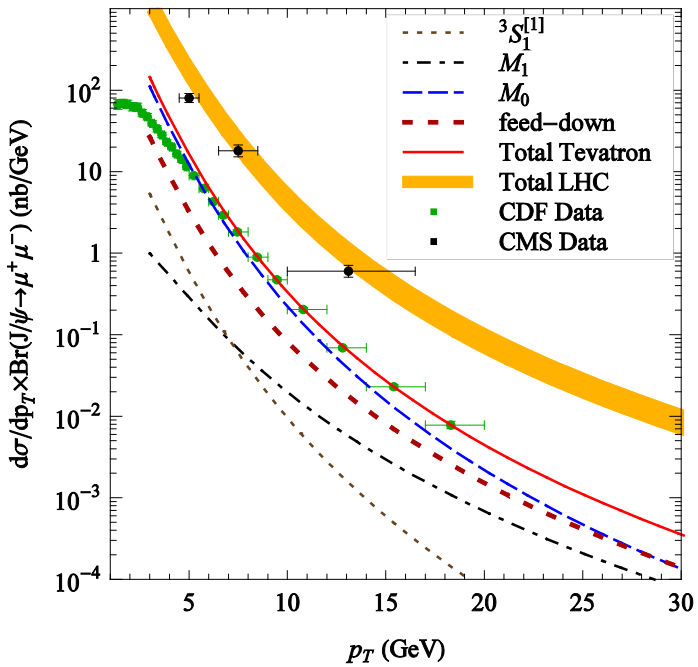

Uncertainty: p_T^{cut}

- In the fit procedure, we abandon data with p_T<7GeV, **which is essential in our work**. There are various reasons for this p_T cut:

✓ Theoretically:

(1) Small p_T region is dominated by non-perturbative effect because of initial state gluon showers (*E.L. Berger et.al. 2005*).

(2) NRQCD factorization is still not proven. But for large p_T region, it was found the factorization holds up to $O(m^4/p_T^4)$ correction (*Z.B. Kang et.al. 2011*). So data in large p_T are more confident to describe.

✓ Experimentally: In the plot, the curvature of data curve is positive at large p_T but negative at small p_T, with a turning point at $p_T \approx 6\ GeV$. Thus data below 7GeV cannot be described by perturbative factorization theory.

✓ Fit: We perform a χ^2 analysis for J/ψ, and find χ^2/d.o.f. decreases rapidly as the cut increases from 3GeV to 7GeV, and then it almost unchanges when the cut becomes larger:

lower p_T cut (Gev)	χ^2/dof	$<O^3S_1^{[8]}>_{J/\psi}$	$<O^1S_0^{[8]}>_{J/\psi}$
3	236.269/16=14.7668	0.360089	1.78736
4	92.9272/12=7.74393	0.250964	3.49161
5	27.8681/8=3.48351	0.157748	5.1679
6	9.07871/6=1.51312	0.101501	6.28956
7	1.31256/4=0.328141	0.0492096	7.43362
8	0.817308/3=0.272436	0.037283	7.71245
9	0.434183/2=0.217091	0.0226552	8.07939
10	0.424269/1=0.424269	0.0192824	8.17001

Uncertainty: decomposition (1)

$$d\hat{\sigma}[^3P_J^{[8]}]=r_0\, d\hat{\sigma}[^1S_0^{[8]}]+r_1\, d\hat{\sigma}[^3S_1^{[8]}]$$

- Two errors induced by decomposing the P-wave channel:
  1) The decomposition has an error of a few percent;
  2) The resulted r_0 and r_1 vary for different experimental condition.
- The above uncertainties can be determined by using three unconstrained LDMEs to fit data (*we thank G. Bodwin for pointing out this*). Choosing p_T^{cut}=7GeV and by minimizing χ^2 we get:

$$O_1 \equiv \langle \mathcal{O}^{J/\psi}(^1S_0^{[8]})\rangle = \quad 15.7\times 10^{-2} GeV^3 (\pm 129\%)$$
$$O_2 \equiv \langle \mathcal{O}^{J/\psi}(^3S_1^{[8]})\rangle = -1.18\times 10^{-2} GeV^3 (\pm 249\%)$$
$$O_3 \equiv \frac{\langle \mathcal{O}^{J/\psi}(^3P_0^{[8]})\rangle}{m_c^2} = -2.28\times 10^{-2} GeV^3 (\pm 239\%)$$

- These LDMEs are obviously unphysically determined. Physical variables are eigenvectors of correlation matrix, which corresponds to linear combinations of these LDMEs:

$$\begin{pmatrix}\Lambda_1\\ \Lambda_2\\ \Lambda_3\end{pmatrix} = \begin{pmatrix}0.96 & -0.14 & -0.26\\ 0.29 & 0.31 & 0.91\\ 0.047 & 0.94 & -0.33\end{pmatrix}\begin{pmatrix}O_1\\ O_2\\ O_3\end{pmatrix} = \begin{pmatrix}15.8\pm 134\%\\ 2.11\pm 5.13\%\\ 0.39\pm 2.45\%\end{pmatrix}\times 10^{-2} GeV^3$$

Comparison:

$$\vec{\mathbf{v}}_{\mathrm{M}_0} = (0.25 \quad 0 \quad 0.97)$$
$$\vec{\mathbf{v}}_{\mathrm{M}_1} = (0 \quad 0.87 \quad -0.48)$$

$M_{0,r_0}^{J/\psi}$ and $M_{1,r_1}^{J/\psi}$ are approximately equivalent to the two well constrained LDMEs:

$$\Lambda_2 \leftrightarrow \mathrm{M}_0$$
$$\Lambda_3 \leftrightarrow \mathrm{M}_1$$

Uncertainty: decomposition (2)

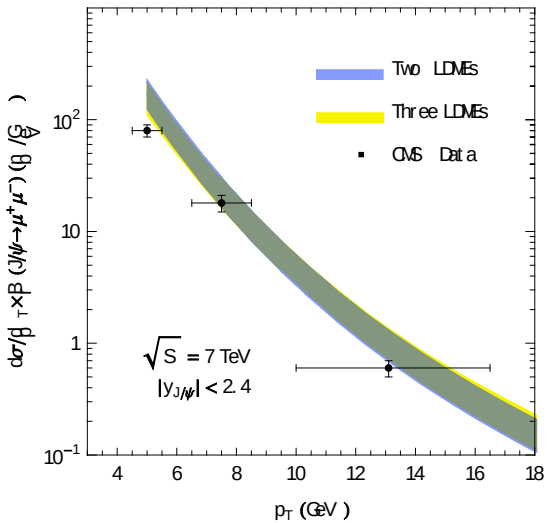

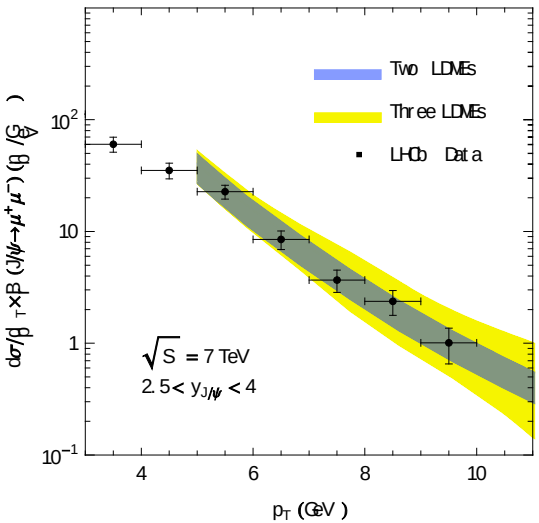

- Predictions between using two LDMEs method and three LDMEs implies:
  1) In central region, two methods give almost the same error bar;
  2) In forward region, three LDMEs method has larger error bar, which means two LDMEs method may underestimates its theoretical uncertainty. (It is interesting to note that the data still seems to locate within the error bar of two LDMEs method predictions.)
- Reason: r_i have small differences between CMS and CDF, but larger difference between LHCb and CDF.
- **It is possible to determine all three LDMEs when data in forward region are sufficient enough!**

Uncertainty: feeddown

- Feeddown contribution mainly from ψ(2S) and χ_{cJ} , all of which are calculated to NLO and their CO LDMEs are determined by fit Tevatron data.
- The transverse momentum difference is considered and approximated as:

$$p_T^{J/\psi} \approx p_T^H \times \frac{m_{J/\psi}}{m_H}$$

with an very small error $O(\frac{(m_{J/\psi}-m_H)^2}{m_H^2})$. (*We thank J.P. Lansberg and P. Faccioli for helping to test this approximation by simulation.*)

Comparison: If we assume the feeddown from ψ(2S) and χ_{cJ} is a constant for all pT region, e.g. 36%, the results change small:

Using three LDMEs: (36% feeddown)

$$M_{0,r_0}^{J/\psi} = 5.47 \times 10^{-2} GeV^3 (\pm 12\%)$$
$$M_{1,r_1}^{J/\psi} = 0.107 \times 10^{-2} GeV^3 (\pm 63\%)$$

Using two LDMEs: (36% feeddown)

$$M_{0,r_0}^{J/\psi} = 5.71 \times 10^{-2} GeV^3 (\pm 4.4\%)$$
$$M_{1,r_1}^{J/\psi} = 0.08 \times 10^{-2} GeV^3 (\pm 18\%)$$

Using two LDMEs: (default)

$$M_{0,r_0}^{J/\psi} = 7.4 \times 10^{-2} GeV^3 (\pm 5.5\%)$$
$$M_{1,r_1}^{J/\psi} = 0.05 \times 10^{-2} GeV^3 (\pm 45\%)$$

Comparing with Butenschön and Kniehl's work

- Butenschön and Kniehl (BK) do a similar work for J/ ψ production (*see Butenschön's talk*), differences from ours include:
  1) BK use both Tevatron data (p_T^{cut}=3GeV) and HERA data (p_T^{cut}=1GeV) ;
  2) BK neglect the feeddown contribution;
  3) BK determine all three CO LDMEs.
- To take advantage of their results, we also neglect feeddown contribution and using three LDMEs to fit (because these choices do not change final results qualitatively, as discussed above), but we still use only Tevatron data with p_T^{cut}=7GeV.

BK's results (errors may be smaller than 10%):

$$M_{0,r_0}^{J/\psi} = 2.47 \times 10^{-2} GeV^3$$
$$M_{1,r_1}^{J/\psi} = 0.594 \times 10^{-2} GeV^3$$

Our results:

$$M_{0,r_0}^{J/\psi} = 8.54 \times 10^{-2} GeV^3 (\pm 12\%)$$
$$M_{1,r_1}^{J/\psi} = 0.167 \times 10^{-2} GeV^3 (\pm 63\%)$$

- $M_{0,r_0}^{J/\psi}$ is well constrained in both two groups, but two results are different significantly. Only difference: using different data!!!

★ Observation: **perturbative NRQCD factorization cannot give a consistent description of both** Tevatron data (7GeV > p_T >3GeV) + HERA data (p_T >1GeV) and Tevatron data (p_T >7GeV).

J/Ψ@LHC mid. p_T (1)

Y. Q.Ma, K.Wang, KTC (2010)

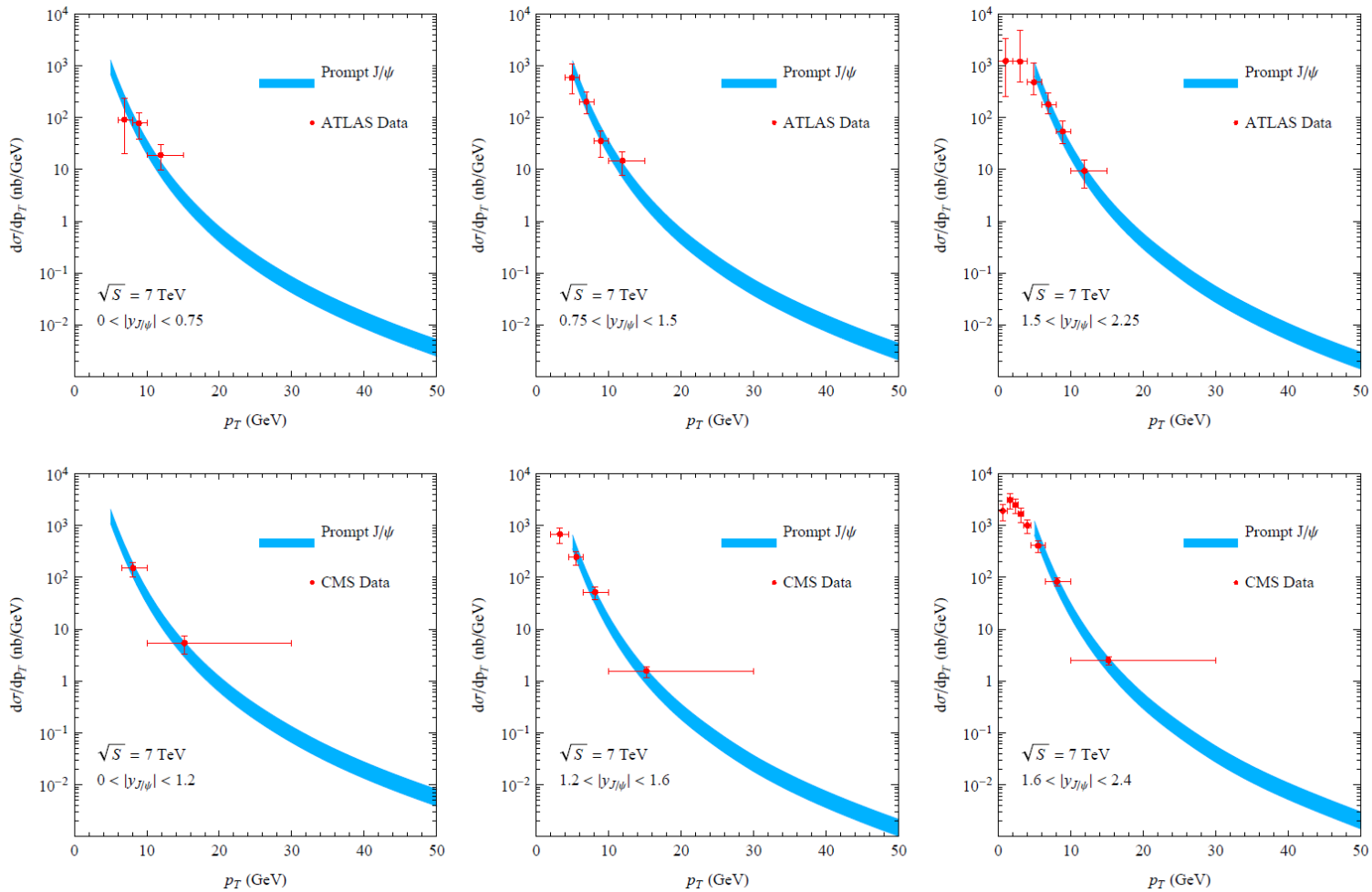

J/Ψ@LHC mid. p_T (2)

Y. Q.Ma, K.Wang, KTC (2010)

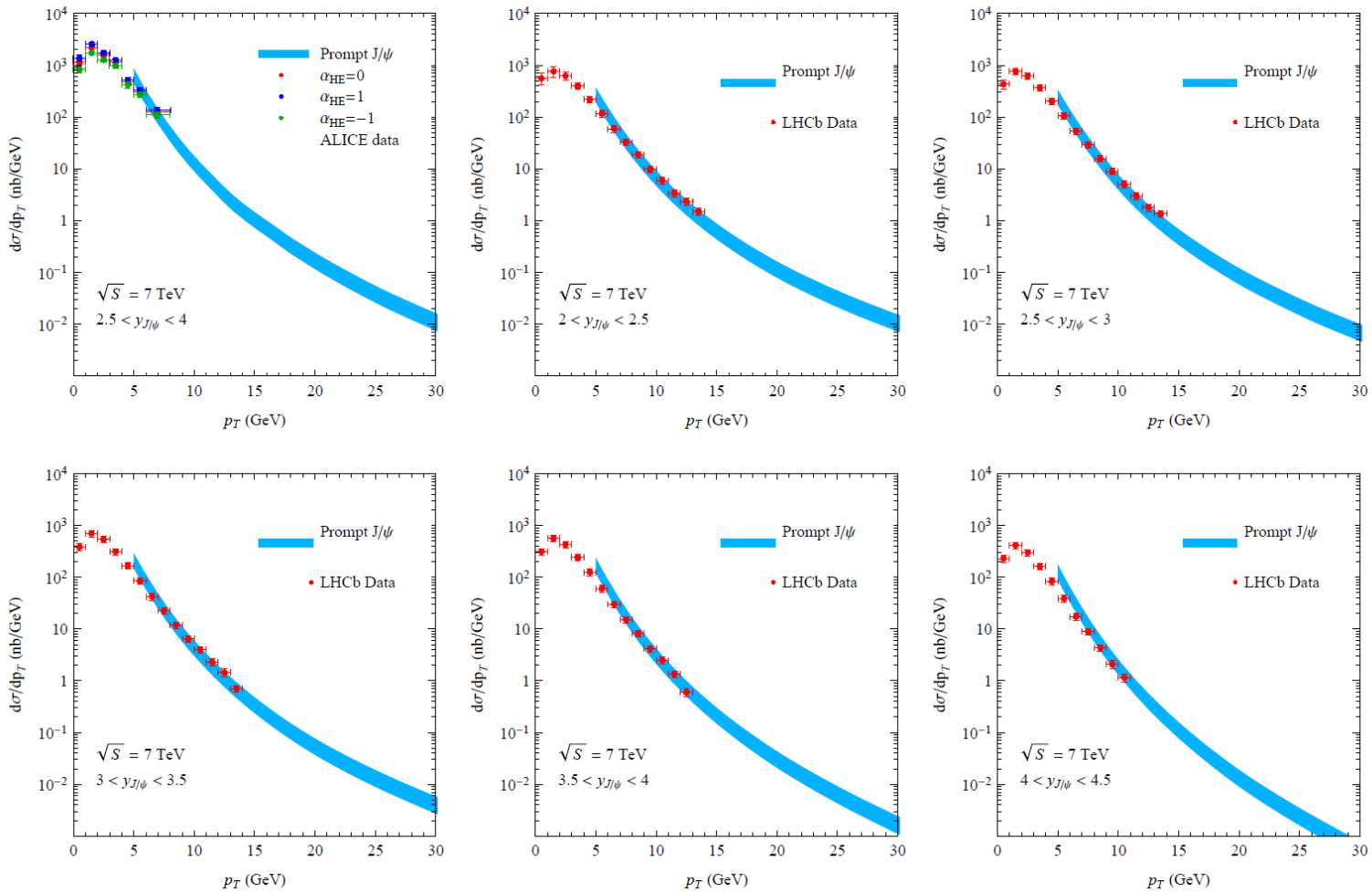

J/Ψ@LHC LARGE p_T

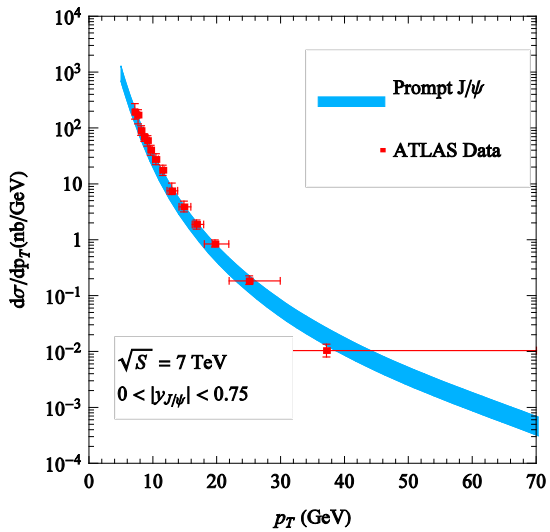

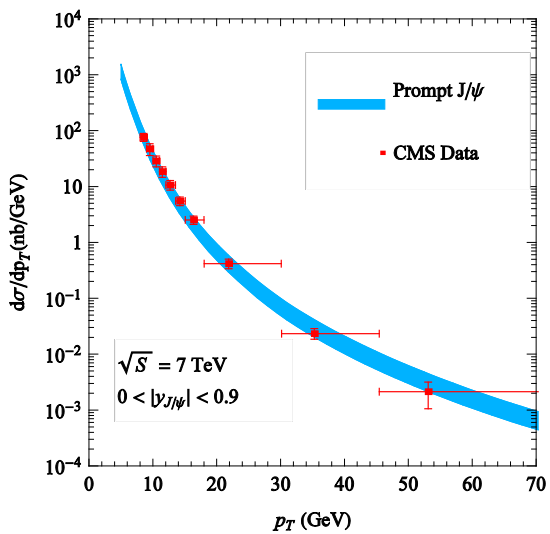

- Data at high p_T: very important to distinguish between different models.
- Our predictions agree with large p_T data, all data can be described by theory within the uncertainty of a factor of two.
- Fit parameters using Tevatron data with 7< p_T <20GeV, predict LHC up to p_T =70GeV, nontrivial!
- It is needed to determine CO LDMEs from these large p_T data when data are adequate enough.

Ψ(2S)@LHC

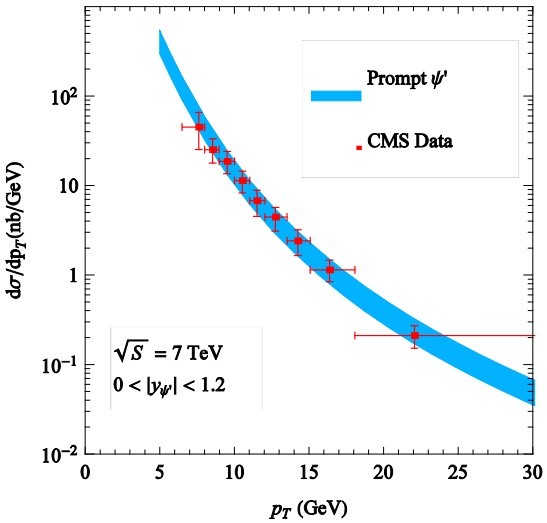

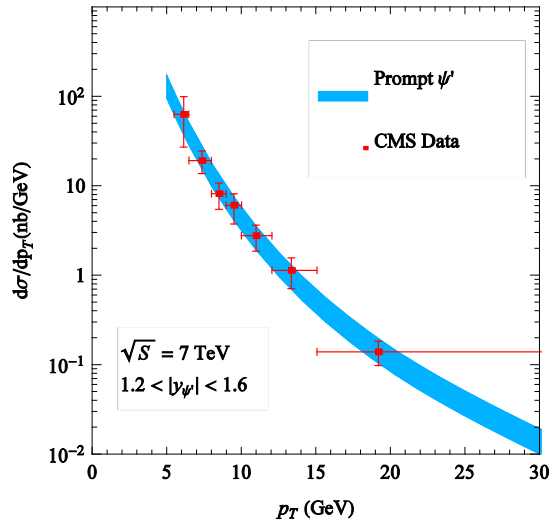

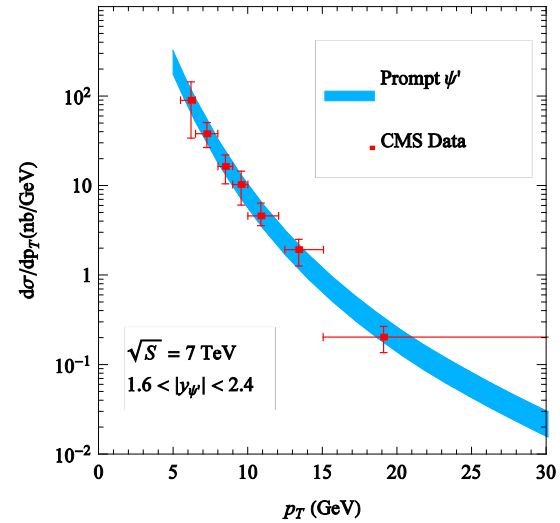

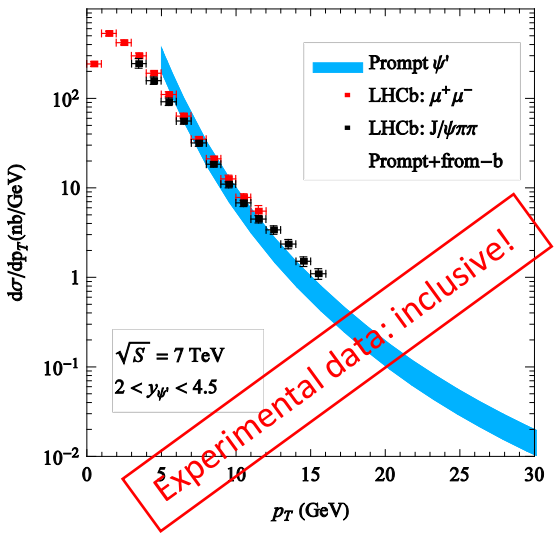

- Fit parameters of Ψ(2S) using Tevatron data.
- Predictions are in good agreement with CMS data.

ϒ(1S)@LHC (1)

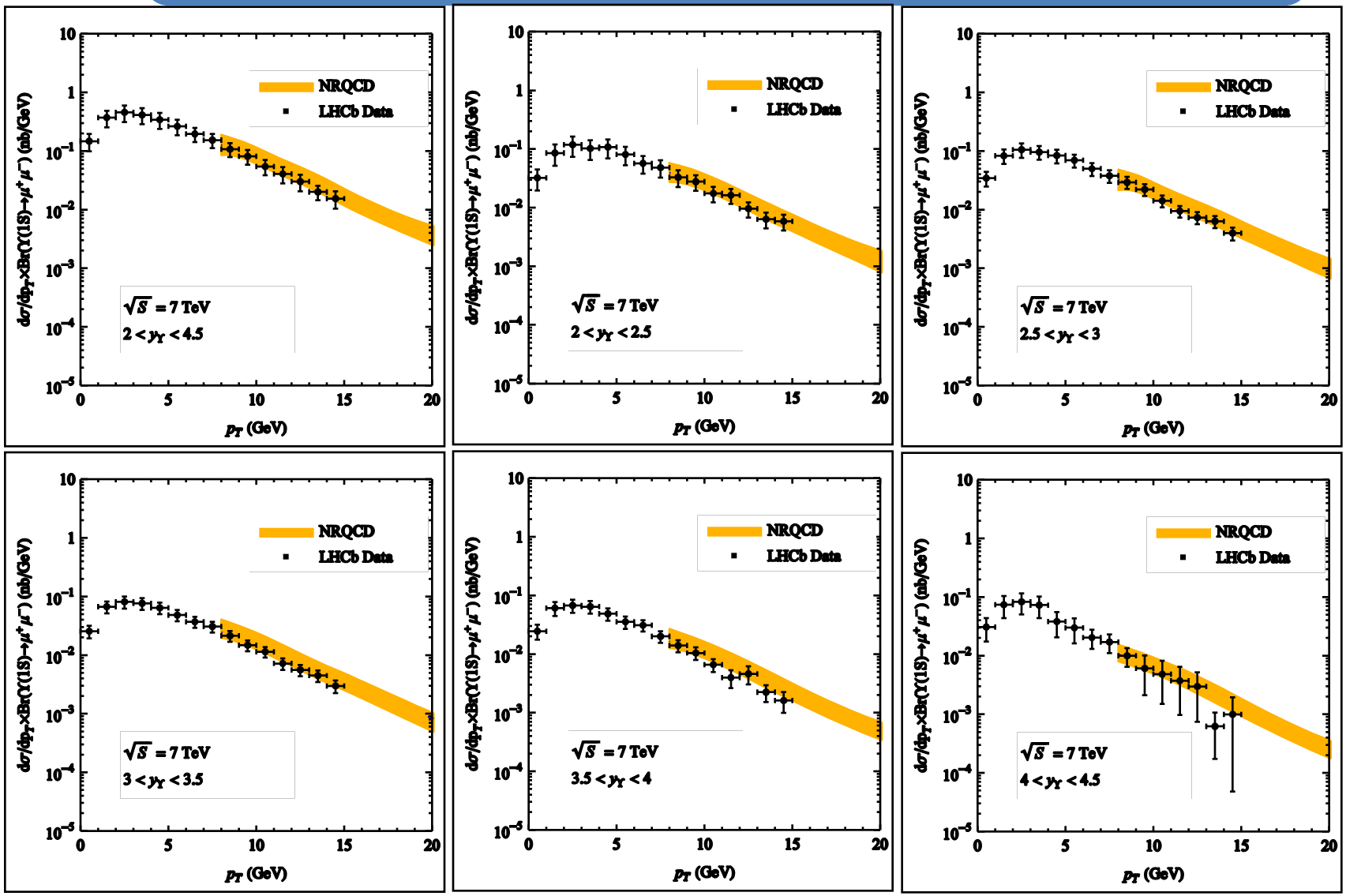

K.Wang, Y.Q.Ma, KTC (2012)

ϒ(1S)@LHC (2)

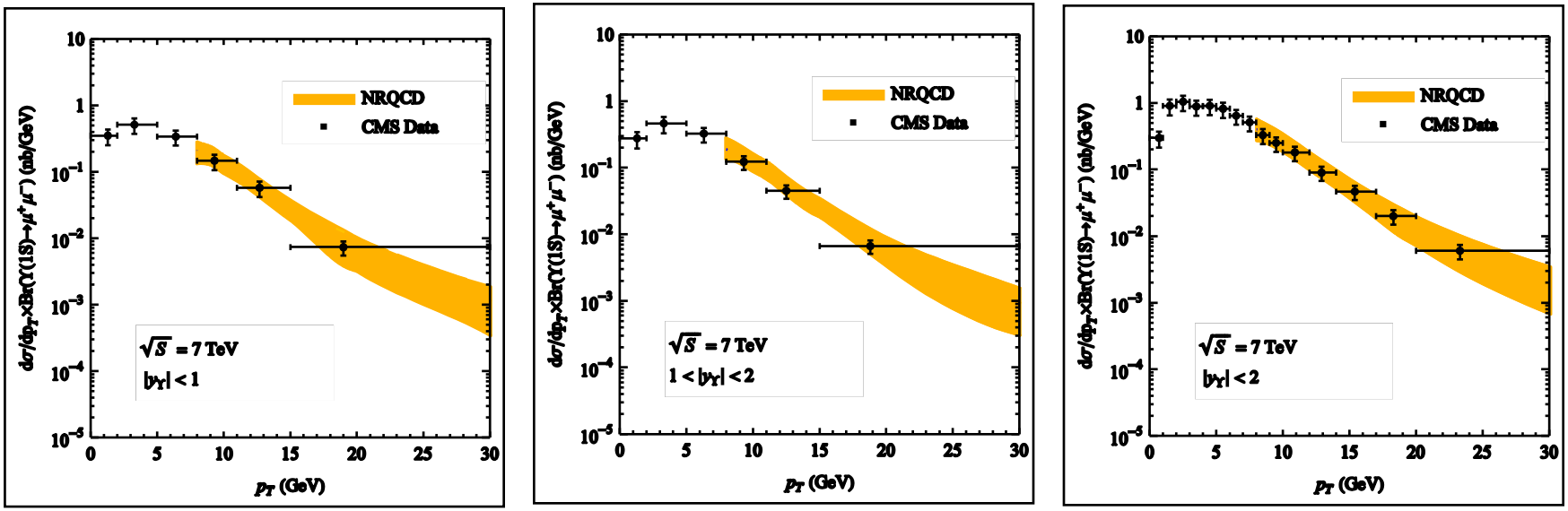

- Fit parameters of ϒ(1S) using Tevatron data.
- Predictions for LHC: good agreement.
- Large error bar in the prediction: large uncertainty of CO LDMEs because p_T region of Tevatron data is too small.

K.Wang, Y.Q.Ma, KTC (2012)

Heavy Quarkonia@RHIC

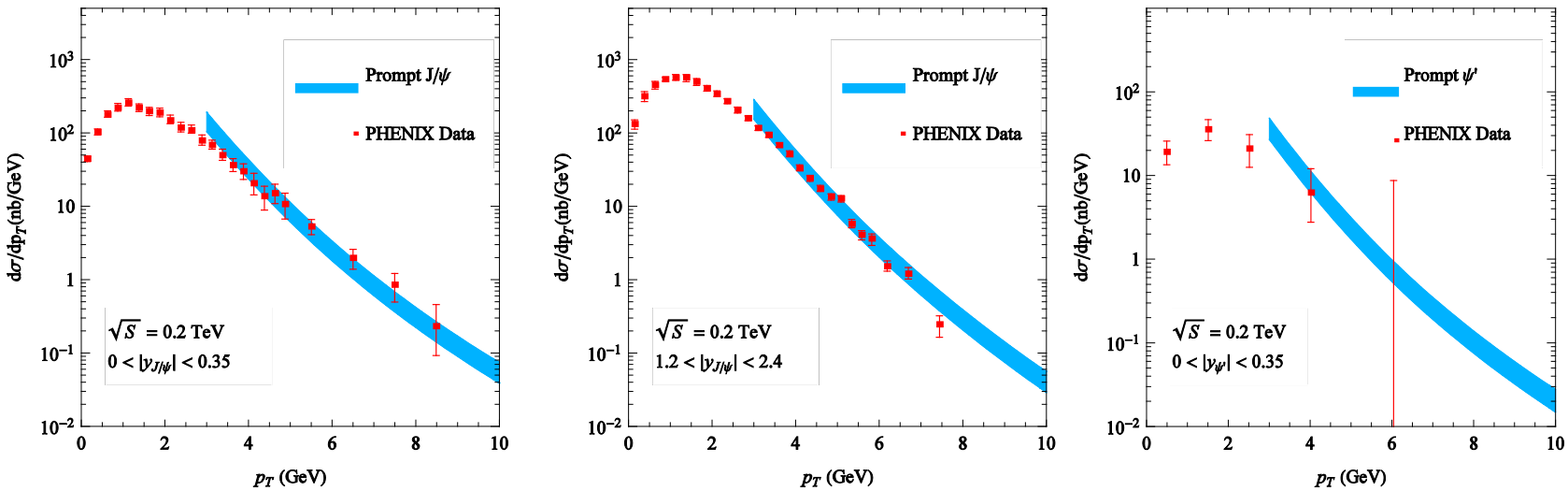

- Good agreement with RHIC data for both J/ Ψ and Ψ(2S).
- Curvature turn point in RHIC: about p_T =3GeV.
- Non-perturbative effect may be important at p_T =3GeV even for $\sqrt{S}$=0.2TeV.

χc @ Tevatron

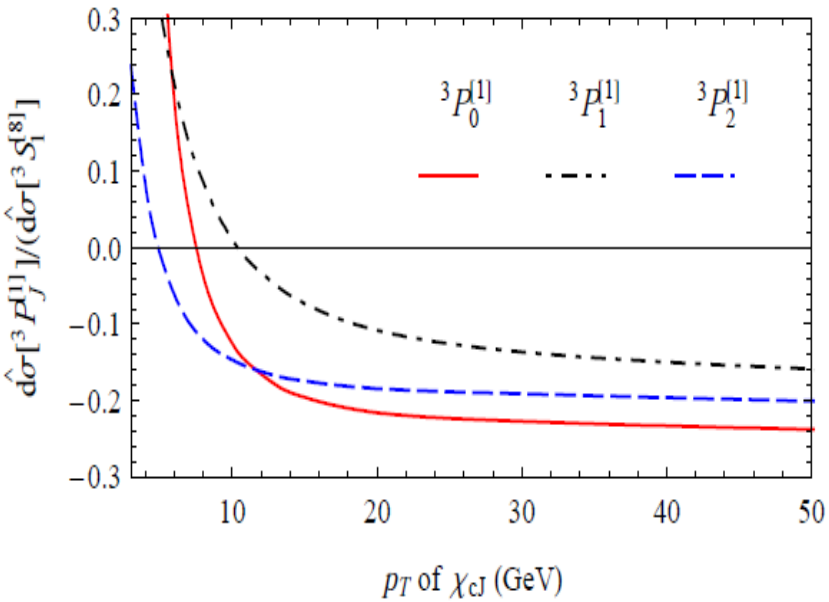

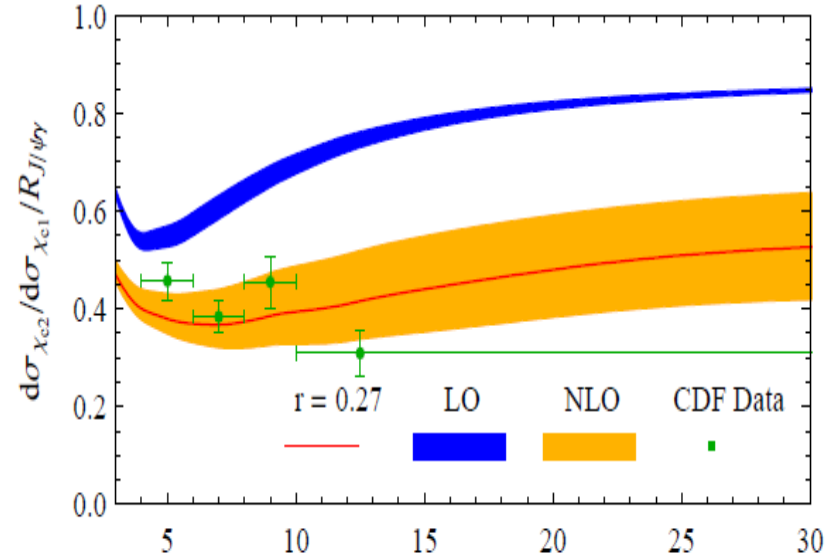

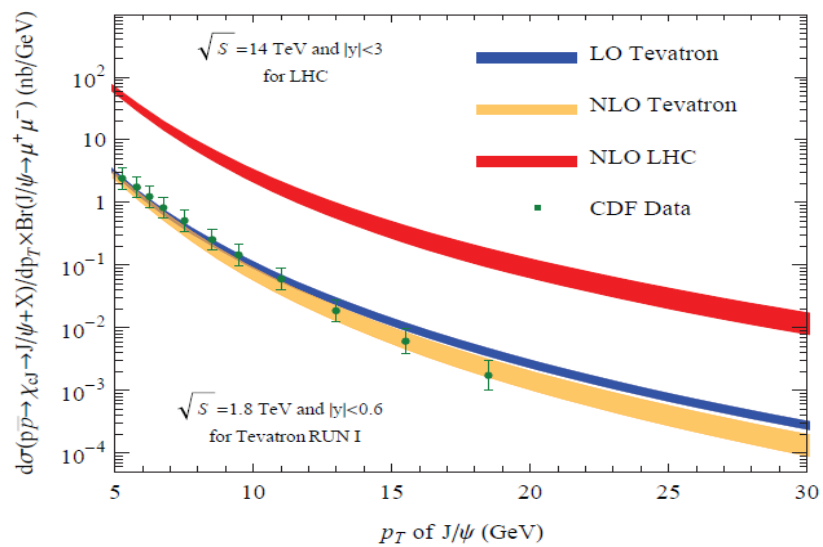

Y. Q.Ma, K.Wang, KTC (2010)

- The fact that at NLO $^3P_1^{[1]}$ decreases slower than $^3P_2^{[1]}$ as pT increases provides an opportunity to lower the value of R.
- By fitting the CDF data, we extract CO long distance matrix element $\langle O^{\chi_{c0}}(^3S_1^{[8]})\rangle = (2.2 \pm 0.48)\times 10^{-3} GeV^3$
- Both cross section and R are described well !

χc @ LHC

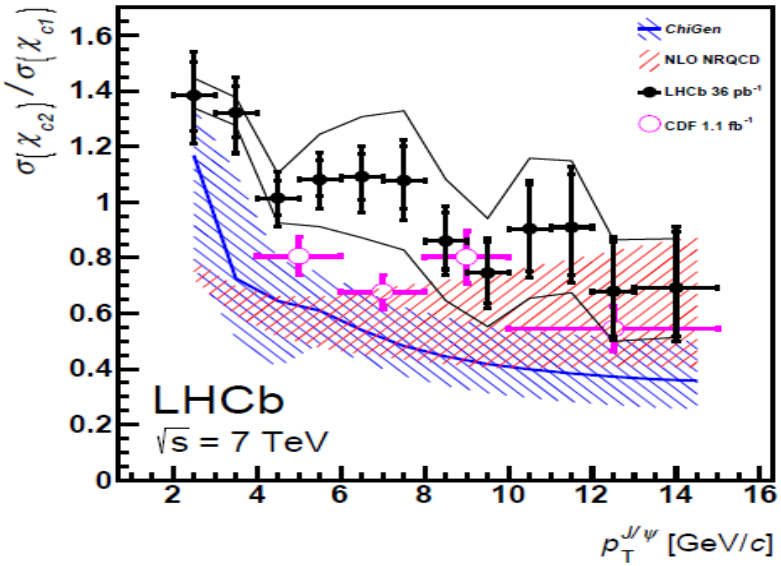

LHCb collaboration (2012)

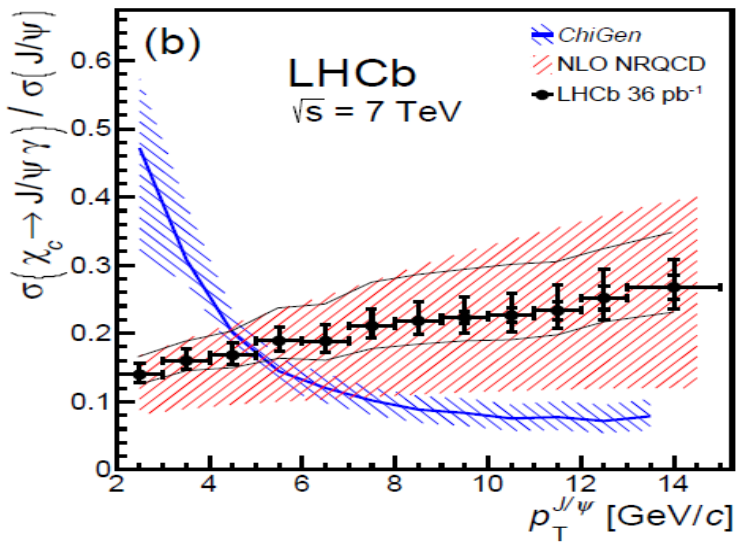

LHCb collaboration (2012)

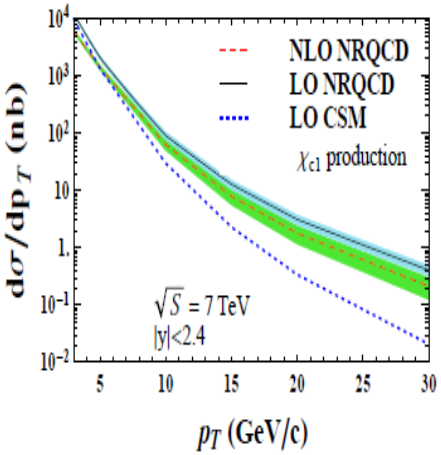

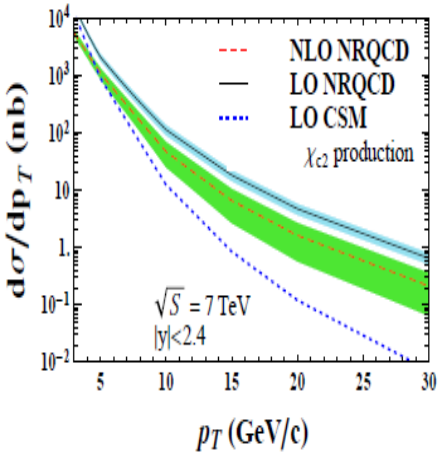

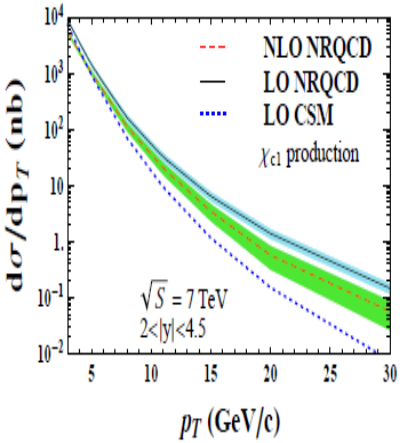

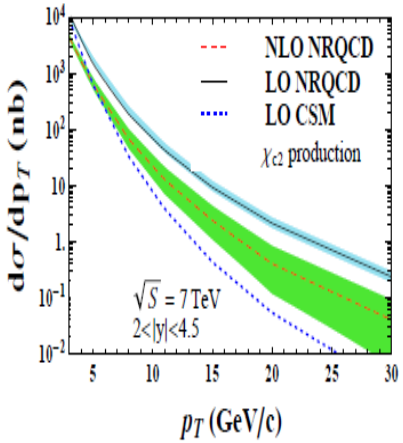

Polarizations

Angular distributions: spin-1

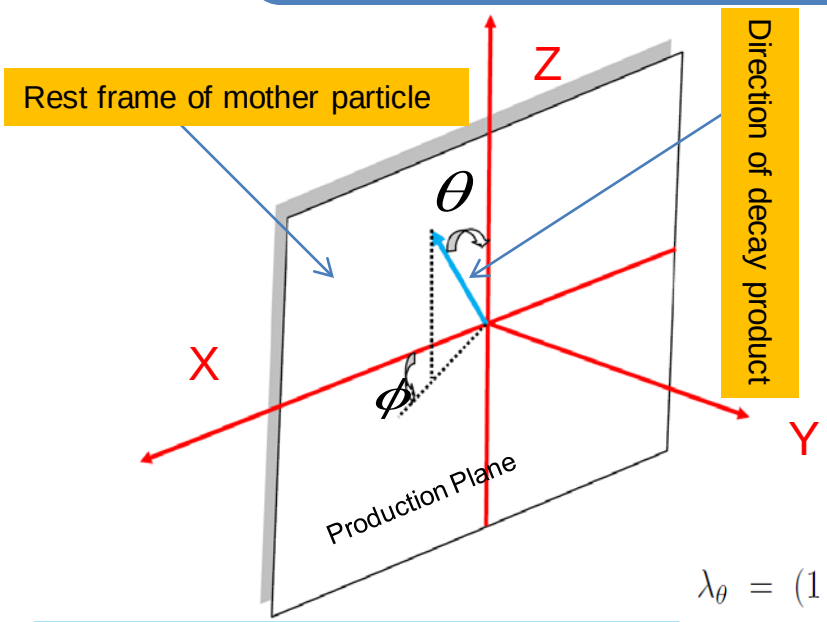

H.S.Shao, KTC (in preparation)

- Spin-1 boson:

$$\mathcal{W}^V(\theta,\phi) \propto 1+\lambda_\theta\cos^2\theta+\lambda_\phi\sin^2\theta\cos\phi + \lambda_{\theta\phi}\sin 2\theta\cos\phi+\lambda_\phi^\perp\sin^2\theta\sin 2\phi + \lambda_{\theta\phi}^\perp\sin 2\theta\sin\phi+2\eta_\theta\cos\theta + 2\eta_{\theta\phi}\sin\theta\cos\phi+2\eta_{\theta\phi}^\perp\sin\theta\sin\phi,$$

$$\lambda_\theta = (1-3\delta)\frac{N_V-3\rho^V_{0,0}}{(1+\delta)N_V+(1-3\delta)\rho^V_{0,0}},\quad \lambda_{\theta\phi}^\perp = -(1-3\delta)\frac{\sqrt{2}(\Im\rho^V_{1,0}+\Im\rho^V_{-1,0})}{(1+\delta)N_V+(1-3\delta)\rho^V_{0,0}},$$

$$\lambda_\phi = (1-3\delta)\frac{2\Re\rho^V_{1,-1}}{(1+\delta)N_V+(1-3\delta)\rho^V_{0,0}},\quad \eta_\theta = \alpha\frac{\rho^V_{1,1}-\rho^V_{-1,-1}}{(1+\delta)N_V+(1-3\delta)\rho^V_{0,0}},$$

$$\lambda_{\theta\phi} = (1-3\delta)\frac{\sqrt{2}(\Re\rho^V_{1,0}-\Re\rho^V_{-1,0})}{(1+\delta)N_V+(1-3\delta)\rho^V_{0,0}},\quad \eta_{\theta\phi} = \alpha\frac{\sqrt{2}(\Re\rho^V_{1,0}+\Re\rho^V_{-1,0})}{(1+\delta)N_V+(1-3\delta)\rho^V_{0,0}},$$

$$\lambda_\phi^\perp = -(1-3\delta)\frac{2\Im\rho^V_{1,-1}}{(1+\delta)N_V+(1-3\delta)\rho^V_{0,0}},\quad \eta_{\theta\phi}^\perp = -\alpha\frac{\sqrt{2}(\Im\rho^V_{1,0}-\Im\rho^V_{-1,0})}{(1+\delta)N_V+(1-3\delta)\rho^V_{0,0}},$$

$$N_V = \rho^V_{1,1}+\rho^V_{0,0}+\rho^V_{-1,-1},$$

- There are two parameters α and δ to be determined by the specific decay process.
- α is vanishing unless parity is violated.
- For J/ψ decays into two massless fermions, $\delta = 0$.
- For χ_{c1} decays into a photon and a J/ψ, $\delta = \frac{1+2a_1^{J=1}a_2^{J=1}}{2}$, where $a_1^{J=1}, a_2^{J=1}$ are the normalized E1 and M2 amplitudes

Angular distributions: spin-2

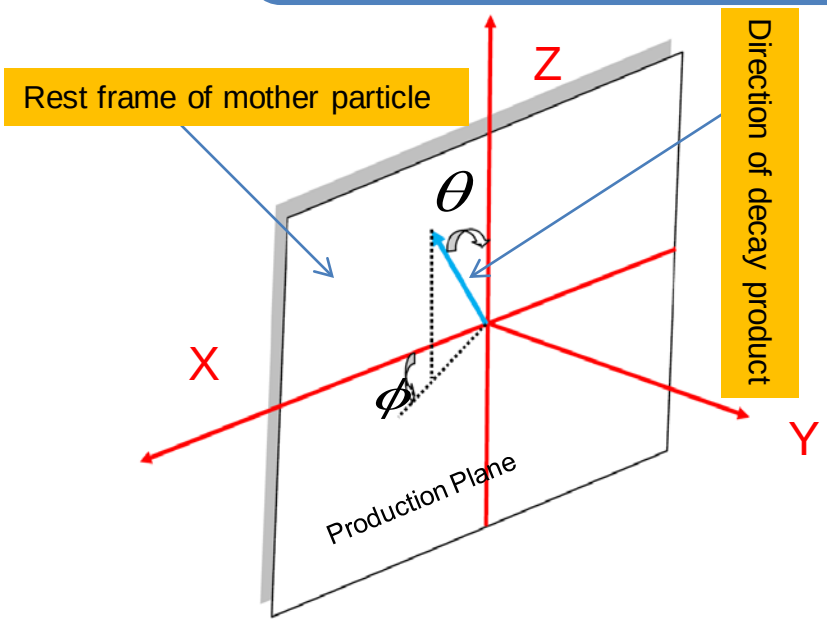

H.S.Shao, KTC (in preparation)

- Spin-2 boson:

$$
\begin{aligned}
\mathcal{W}^{T_2}(\theta,\phi) \propto\ & 1+\lambda_\theta\cos^2\theta+\lambda_{2\theta}\cos^4\theta \\
&+\lambda_{\theta\phi}\sin 2\theta\cos\phi+\lambda_{2\theta\phi}\sin 2\theta\sin^2\theta\cos\phi \\
&+\lambda^{\perp}_{\theta\phi}\sin 2\theta\sin\phi+\lambda^{\perp}_{2\theta\phi}\sin 2\theta\sin^2\theta\sin\phi \\
&+\lambda_{\phi}\sin^2\theta\cos 2\phi+\lambda_{2\phi}\sin^4\theta\cos 2\phi \\
&+\lambda^{\perp}_{\phi}\sin^2\theta\sin 2\phi+\lambda^{\perp}_{2\phi}\sin^4\theta\sin 2\phi \\
&+\lambda_{3\theta\phi}\sin 2\theta\sin^2\theta\cos 3\phi \\
&+\lambda^{\perp}_{3\theta\phi}\sin 2\theta\sin^2\theta\sin 3\phi \\
&+\lambda_{4\phi}\sin^4\theta\cos 4\phi+\lambda^{\perp}_{4\phi}\sin^4\theta\sin 4\phi \\
&+2\eta_\theta\cos\theta+2\eta_{2\theta}\cos^3\theta \\
&+2\eta_{\theta\phi}\sin\theta\cos\phi+2\eta_{2\theta\phi}\sin^3\theta\cos\phi \\
&+2\eta^{\perp}_{\theta\phi}\sin\theta\sin\phi+2\eta^{\perp}_{2\theta\phi}\sin^3\theta\sin\phi \\
&+2\eta_{\phi}\sin^2\theta\cos\theta\cos 2\phi+2\eta^{\perp}_{\phi}\sin^2\theta\cos\theta\sin 2\phi \\
&+2\eta_{3\theta\phi}\sin^3\theta\cos 3\phi \\
&+2\eta^{\perp}_{3\theta\phi}\sin^3\theta\sin 3\phi, \qquad \text{(B1)}
\end{aligned}
$$

$$
\begin{aligned}
\lambda_\theta &= 6[(1-3\delta_0-\delta_1)N_{T_2} \\
&- (1-7\delta_0+\delta_1)(\rho^{T_2}_{1,1}+\rho^{T_2}_{-1,-1}) \\
&- (3-\delta_0-7\delta_1)\rho^{T_2}_{0,0}]/R, \\
\lambda_{2\theta} &= (1+5\delta_0-5\delta_1)[N_{T_2}-5(\rho^{T_2}_{1,1}+\rho^{T_2}_{-1,-1} \\
&+ 5\rho^{T_2}_{0,0}]/R, \\
\lambda_{\theta\phi} &= 4[2(1-\delta_0-2\delta_1)(\Re\rho^{T_2}_{2,1}-\Re\rho^{T_2}_{-2,-1}) \\
&- \sqrt{6}(2\delta_0-\delta_1)(\Re\rho^{T_2}_{1,0}-\Re\rho^{T_2}_{-1,0})]/R, \\
\lambda_{2\theta\phi} &= -2(1+5\delta_0-5\delta_1)[(\Re\rho^{T_2}_{2,1}-\Re\rho^{T_2}_{-2,-1}) \\
&- \sqrt{6}(\Re\rho^{T_2}_{1,0}-\Re\rho^{T_2}_{-1,0})]/R, \\
\lambda^{\perp}_{\theta\phi} &= 4[-2(1-\delta_0-2\delta_1)(\Im\rho^{T_2}_{2,1}+\Im\rho^{T_2}_{-2,-1}) \\
&+ \sqrt{6}(2\delta_0-\delta_1)(\Im\rho^{T_2}_{1,0}+\Im\rho^{T_2}_{-1,0})]/R, \\
\lambda^{\perp}_{2\theta\phi} &= 2(1+5\delta_0-5\delta_1)[(\Im\rho^{T_2}_{2,1}+\Im\rho^{T_2}_{-2,-1}) \\
&- \sqrt{6}(\Im\rho^{T_2}_{1,0}+\Im\rho^{T_2}_{-1,0})]/R,
\end{aligned}
$$

Angular distributions: spin-2

$$
\begin{aligned}
\eta_\theta &= 2[(2\alpha_1+\alpha_2)(\rho^{T_2}_{2,2}-\rho^{T_2}_{-2,-2}) \\
&- 2(\alpha_1-\alpha_2)(\rho^{T_2}_{1,1}-\rho^{T_2}_{-1,-1})]/R, \\
\eta_{2\theta} &= -2(2\alpha_1-\alpha_2)[(\rho^{T_2}_{2,2}-\rho^{T_2}_{-2,-2}) \\
&- 2(\rho^{T_2}_{1,1}-\rho^{T_2}_{-1,-1})]/R, \\
\eta_{\theta\phi} &= -4[2(\alpha_1-\alpha_2)(\Re\rho^{T_2}_{2,1}+\Re\rho^{T_2}_{-2,-1}) \\
&- \sqrt{6}\alpha_1(\Re\rho^{T_2}_{1,0}+\Re\rho^{T_2}_{-1,0})]/R, \\
\eta_{2\theta\phi} &= 2(2\alpha_1-\alpha_2)[3(\Re\rho^{T_2}_{2,1}+\Re\rho^{T_2}_{-2,-1}) \\
&- \sqrt{6}(\Re\rho^{T_2}_{1,0}+\Re\rho^{T_2}_{-1,0})]/R, \\
\eta^\perp_{\theta\phi} &= 4[2(\alpha_1-\alpha_2)(\Im\rho^{T_2}_{2,1}-\Im\rho^{T_2}_{-2,-1}) \\
&- \sqrt{6}\alpha_1(\Im\rho^{T_2}_{1,0}-\Im\rho^{T_2}_{-1,0})]/R, \\
\eta^\perp_{2\theta\phi} &= -2(2\alpha_1-\alpha_2)[3(\Im\rho^{T_2}_{2,1}-\Im\rho^{T_2}_{-2,-1}) \\
&- \sqrt{6}(\Im\rho^{T_2}_{1,0}-\Im\rho^{T_2}_{-1,0})]/R, \\
\eta_\phi &= -2\sqrt{6}(2\alpha_1-\alpha_2)\frac{\Re\rho^{T_2}_{2,0}-\Re\rho^{T_2}_{-2,0}}{R}, \\
\eta^\perp_\phi &= 2\sqrt{6}(2\alpha_1-\alpha_2)\frac{\Im\rho^{T_2}_{2,0}+\Im\rho^{T_2}_{-2,0}}{R}, \\
\eta_{3\theta\phi} &= -2(2\alpha_1-\alpha_2)\frac{\Re\rho^{T_2}_{2,-1}+\Re\rho^{T_2}_{-2,1}}{R}, \\
\eta^\perp_{3\theta\phi} &= 2(2\alpha_1-\alpha_2)\frac{\Im\rho^{T_2}_{2,-1}-\Im\rho^{T_2}_{-2,1}}{R},
\end{aligned}
$$

$$
\begin{aligned}
\lambda_\phi &= 4[\sqrt{6}(1+\delta_0-3\delta_1)(\Re\rho^{T_2}_{2,0}+\Re\rho^{T_2}_{-2,0}) \\
&- 6(2\delta_0-\delta_1)\Re\rho^{T_2}_{1,-1}]/R, \\
\lambda_{2\phi} &= -2(1+5\delta_0-5\delta_1)[\sqrt{6}(\Re\rho^{T_2}_{2,0}+\Re\rho^{T_2}_{-2,0}) \\
&- 4\Re\rho^{T_2}_{1,-1}]/R, \\
\lambda^\perp_\phi &= -4[\sqrt{6}(1+\delta_0-3\delta_1)(\Im\rho^{T_2}_{2,0}-\Im\rho^{T_2}_{-2,0}) \\
&- 6(2\delta_0-\delta_1)\Im\rho^{T_2}_{1,-1}]/R, \\
\lambda^\perp_{2\phi} &= 2(1+5\delta_0-5\delta_1)[\sqrt{6}(\Im\rho^{T_2}_{2,0}-\Im\rho^{T_2}_{-2,0}) \\
&- 4\Im\rho^{T_2}_{1,-1}]/R, \\
\lambda_{3\theta\phi} &= 2(1+5\delta_0-5\delta_1)\frac{\Re\rho^{T_2}_{2,-1}-\Re\rho^{T_2}_{-2,1}}{R}, \\
\lambda^\perp_{3\theta\phi} &= -2(1+5\delta_0-5\delta_1)\frac{\Im\rho^{T_2}_{2,-1}+\Im\rho^{T_2}_{-2,1}}{R}, \\
\lambda_{4\phi} &= 2(1+5\delta_0-5\delta_1)\frac{\Re\rho^{T_2}_{2,-2}}{R}, \\
\lambda^\perp_{4\phi} &= -2(1+5\delta_0-5\delta_1)\frac{\Im\rho^{T_2}_{2,-2}}{R}, \qquad (
\end{aligned}
$$

$$
\begin{aligned}
N_{T_2} &= \rho^{T_2}_{2,2}+\rho^{T_2}_{1,1}+\rho^{T_2}_{0,0}+\rho^{T_2}_{-1,-1}+\rho^{T_2}_{-2,-2}, \\
R &= (1+5\delta_0+3\delta_1)N_{T_2} \\
&+ 3(1-3\delta_0-\delta_1)(\rho^{T_2}_{1,1}+\rho^{T_2}_{-1,-1}) \\
&+ (5-7\delta_0-9\delta_1)\rho^{T_2}_{0,0}.
\end{aligned}
$$

- There are four parameters δ_0 , δ_1 , α_1 and α_2 to be determined by the specific decay process.
- α_1 , α_2 are vanishing until parity is violated.

Angular distributions: cascade decay I

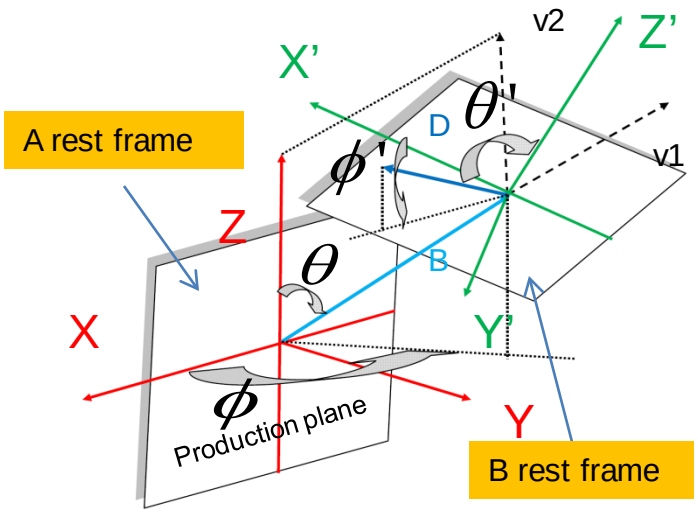

A→B+C
└→ D+E

H.S.Shao, KTC (in preparation)

➢ χ_c with Z'=v1 in $\chi_c \to J/\psi\gamma \to l^+l^-\gamma$

$$\mathcal{W}(\theta',\phi') = \frac{N_{\chi_c}}{3+\lambda_{\theta'}}\Big(1+\lambda_{\theta'}\cos^2\theta' + \lambda_{\phi'}\sin^2\theta'\cos 2\phi' + \lambda_{\theta'\phi'}\sin 2\theta'\cos\phi' + \lambda^{\perp}_{\phi'}\sin^2\theta'\sin 2\phi' + \lambda^{\perp}_{\theta'\phi'}\sin 2\theta'\sin\phi'\Big).$$

$$\lambda^{\chi_{c2}}_{\theta'} = \frac{3(1-11(a_2^{J=2})^2+9(a_3^{J=2})^2)}{39+11(a_2^{J=2})^2-9(a_3^{J=2})^2},$$

$$\lambda^{\chi_{c2}}_{\phi'} = \frac{(a_1^{J=2})^2(7\sqrt{6}(\Re\rho^{\chi_{c2}}_{0,2}+\Re\rho^{\chi_{c2}}_{0,-2})+12\Re\rho^{\chi_{c2}}_{1,-1})}{2(39+11(a_2^{J=2})^2-9(a_3^{J=2})^2)N_{\chi_{c2}}},$$

$$\lambda^{\chi_{c2}}_{\theta'\phi'} = [\sqrt{6}(1-\frac{13}{3}(a_2^{J=2})^2-(a_3^{J=2})^2)(\Re\rho^{\chi_{c2}}_{-1,0}-\Re\rho^{\chi_{c2}}_{1,0}) + 6(4-9(a_2^{J=2})^2-4(a_3^{J=2})^2)(\Re\rho^{\chi_{c2}}_{-2,-1}-\Re\rho^{\chi_{c2}}_{2,1})] / [4(39+11(a_2^{J=2})^2-9(a_3^{J=2})^2)N_{\chi_{c2}}].$$

$$\lambda^{\perp\chi_{c2}}_{\phi'} = \frac{(a_1^{J=2})^2(7\sqrt{6}(\Im\rho^{\chi_{c2}}_{0,2}-\Im\rho^{\chi_{c2}}_{0,-2})-12\Im\rho^{\chi_{c2}}_{1,-1})}{2(39+11(a_2^{J=2})^2-9(a_3^{J=2})^2)N_{\chi_{c2}}},$$

$$\lambda^{\perp\chi_{c2}}_{\theta'\phi'} = [\sqrt{6}(1-\frac{13}{3}(a_2^{J=2})^2-(a_3^{J=2})^2)(\Im\rho^{\chi_{c2}}_{-1,0}+\Im\rho^{\chi_{c2}}_{1,0}) + 6(4-9(a_2^{J=2})^2-4(a_3^{J=2})^2)(\Im\rho^{\chi_{c2}}_{-2,-1}+\Im\rho^{\chi_{c2}}_{2,1})] / [4(39+11(a_2^{J=2})^2-9(a_3^{J=2})^2)N_{\chi_{c2}}].$$

$$\lambda^{\chi_{c1}}_{\theta'} = -\frac{1-3(a_2^{J=1})^2}{3-(a_2^{J=1})^2}, \lambda^{\chi_{c1}}_{\phi'} = \lambda^{\perp\chi_{c1}}_{\phi'} = 0,$$

$$\lambda^{\chi_{c1}}_{\theta'\phi'} = \frac{\sqrt{2}(a_1^{J=1})^2(\Re(\rho^{\chi_{c1}}_{1,0})-\Re(\rho^{\chi_{c1}}_{-1,0}))}{4(3-(a_2^{J=1})^2)N_{\chi_{c1}}},$$

$$\lambda^{\perp\chi_{c1}}_{\theta'\phi'} = -\frac{\sqrt{2}(a_1^{J=1})^2(\Im(\rho^{\chi_{c1}}_{1,0})+\Im(\rho^{\chi_{c1}}_{-1,0}))}{4(3-(a_2^{J=1})^2)N_{\chi_{c1}}},$$

Angular distributions: cascade decay II

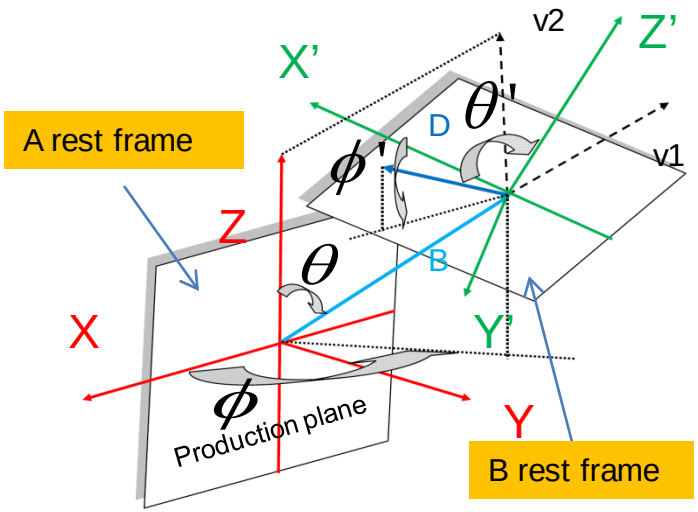

H.S.Shao, KTC (in preparation)

- χ_c with Z'=v2 in $\chi_c \to J/\psi\gamma \to l^+l^-\gamma$

$$\mathcal{W}(\theta',\phi') = \frac{N_{\chi_c}}{3+\lambda_{\theta'}}\Big(1+\lambda_{\theta'}\cos^2\theta' + \lambda_{\phi'}\sin^2\theta'\cos 2\phi' + \lambda_{\theta'\phi'}\sin 2\theta'\cos\phi' + \lambda^{\perp}_{\phi'}\sin^2\theta'\sin 2\phi' + \lambda^{\perp}_{\theta'\phi'}\sin 2\theta'\sin\phi'\Big).$$

A → B+C
└→ D+E

$$\lambda^{\chi_{c2}}_{\theta'} = \frac{6N_{\chi_{c2}} - 9(\rho^{\chi_{c2}}_{1,1}+\rho^{\chi_{c2}}_{-1,-1}) - 12\rho^{\chi_{c2}}_{0,0}}{R_2},$$

$$\lambda^{\chi_{c2}}_{\phi'} = \frac{2\sqrt{6}(\Re\rho^{\chi_{c2}}_{2,0}+\Re\rho^{\chi_{c2}}_{-2,0}) + 6\Re\rho^{\chi_{c2}}_{1,-1}}{R_2},$$

$$\lambda^{\chi_{c2}}_{\theta'\phi'} = \frac{6(\Re\rho^{\chi_{c2}}_{2,1}-\Re\rho^{\chi_{c2}}_{-2,-1}) + \sqrt{6}(\Re\rho^{\chi_{c2}}_{1,0}-\Re\rho^{\chi_{c2}}_{-1,0})}{R_2},$$

$$\lambda^{\perp\chi_{c2}}_{\phi'} = \frac{2\sqrt{6}(\Im\rho^{\chi_{c2}}_{0,2}-\Im\rho^{\chi_{c2}}_{0,-2}) - 6\Im\rho^{\chi_{c2}}_{1,-1}}{R_2},$$

$$\lambda^{\perp\chi_{c2}}_{\theta'\phi'} = \frac{6(\Im\rho^{\chi_{c2}}_{1,2}+\Im\rho^{\chi_{c2}}_{-1,-2}) + \sqrt{6}(\Im\rho^{\chi_{c2}}_{0,1}+\Im\rho^{\chi_{c2}}_{0,-1})}{R_2}$$

$$R_1 = [(15-2(a_2^{J=1})^2)N_{\chi_{c1}} - (5-6(a_2^{J=1})^2)\rho^{\chi_{c1}}_{0,0}]/(5-6(a_2^{J=1})^2),$$

$$R_2 = [2(21+14(a_2^{J=2})^2+5(a_3^{J=2})^2)N_{\chi_{c2}} + 3(7-14(a_2^{J=2})^2-5(a_3^{J=2})^2)(\rho^{\chi_{c2}}_{1,1}+\rho^{\chi_{c2}}_{-1,-1}) + 4(7-14(a_2^{J=2})^2-5(a_3^{J=2})^2)\rho^{\chi_{c2}}_{0,0}] / (7-14(a_2^{J=2})^2-5(a_3^{J=2})^2).$$

$$\lambda^{\chi_{c1}}_{\theta'} = \frac{-N_{\chi_{c1}} + 3\rho^{\chi_{c1}}_{0,0}}{R_1},$$

$$\lambda^{\chi_{c1}}_{\phi'} = -\frac{2\Re\rho^{\chi_{c1}}_{1,-1}}{R_1},$$

$$\lambda^{\chi_{c1}}_{\theta'\phi'} = -\frac{\sqrt{2}(\Re\rho^{\chi_{c1}}_{1,0}-\Re\rho^{\chi_{c1}}_{-1,0})}{R_1},$$

$$\lambda^{\perp\chi_{c1}}_{\phi'} = \frac{2\Im\rho^{\chi_{c1}}_{1,-1}}{R_1},$$

$$\lambda^{\perp\chi_{c1}}_{\theta'\phi'} = \frac{\sqrt{2}(\Im\rho^{\chi_{c1}}_{1,0}+\Im\rho^{\chi_{c1}}_{-1,0})}{R_1},$$

Frames

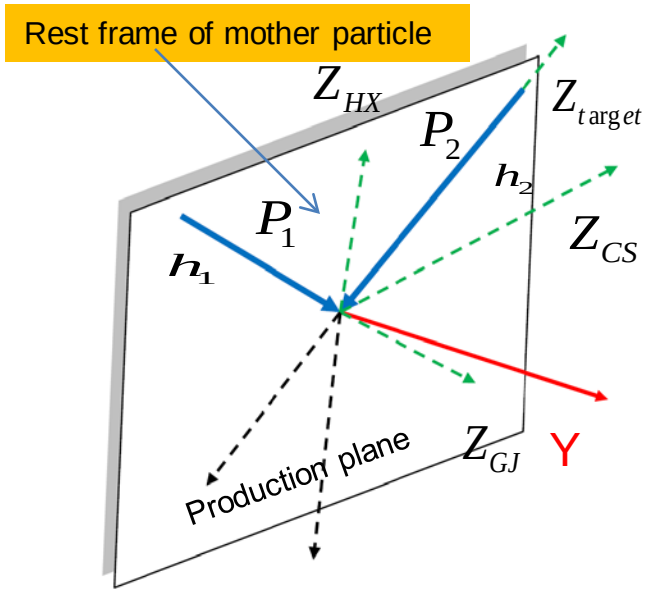

- Helicity frame (HX): $\vec{s} = -(\vec{P}_1 + \vec{P}_2)$
- Collins-Soper frame (CS): $\vec{s} = \vec{P}_1/|\vec{P}_1| - \vec{P}_2/|\vec{P}_2|$
- Gottfried-Jackson frame (GJ): $\vec{s} = \vec{P}_1/|\vec{P}_1|$
- Target frame: $\vec{s} = -\vec{P}_2/|\vec{P}_2|$

- The full spin information should be determined in various frames.
- In high-pT region, the HX and CS are approximated orthogonal.

H.S.Shao, KTC (in preparation)

Q: Is there any frame-independent polarization observable?

- For spin-n boson:

$$F_n \equiv \frac{1}{B_n}\frac{|b_n|^2}{N_n},$$

$$N_n \equiv \sum_{m=-n}^{n} |a_m|^2 \equiv \sum_{m=-n}^{n} \rho_{m,m},$$

$$b_{2k} \equiv \sum^{k} \langle k,m;k,m|2k,2m\rangle a_{2m}, \text{when } n = 2k,$$

$$b_{2k+1} \equiv \sum_{m=0}^{k} \langle 2k+1-m,0;m,0|2k+1,0\rangle (a_{2k+1-m} + a_{m-1-2k}), \text{when } n = 2k+1,$$

The functions of Fn are frame-independent !

Polarization beyond LO in CSM

- J/ψ meson can decay into a lepton pair, and the lepton angular distribution encodes the spin information of J/ψ .
- To solve the polarization J/ψ puzzle, a lot of effort has been made.
- NLO QCD correction to $^3S_1^{[1]}$ channel.
- The color-singlet polarization is changed from being transverse at LO to be longitudinal beyond LO.

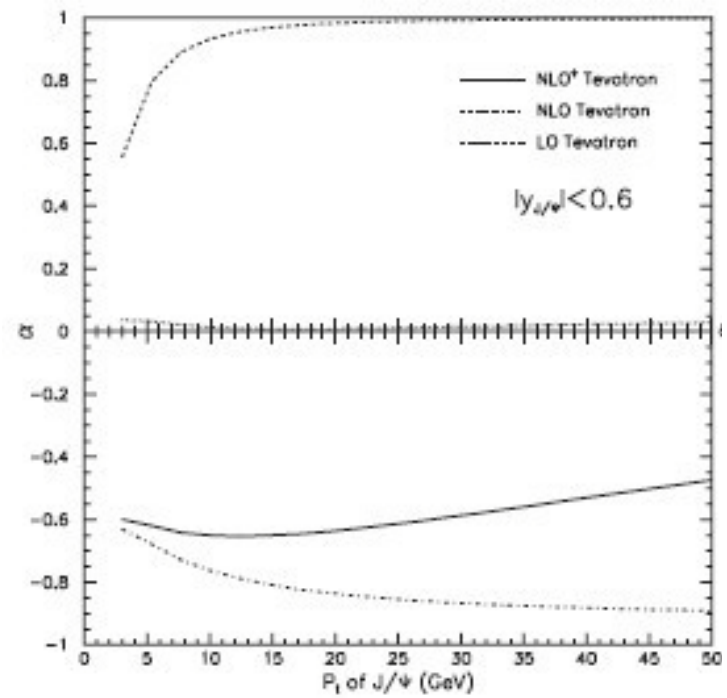

B.Gong et al. (2008)

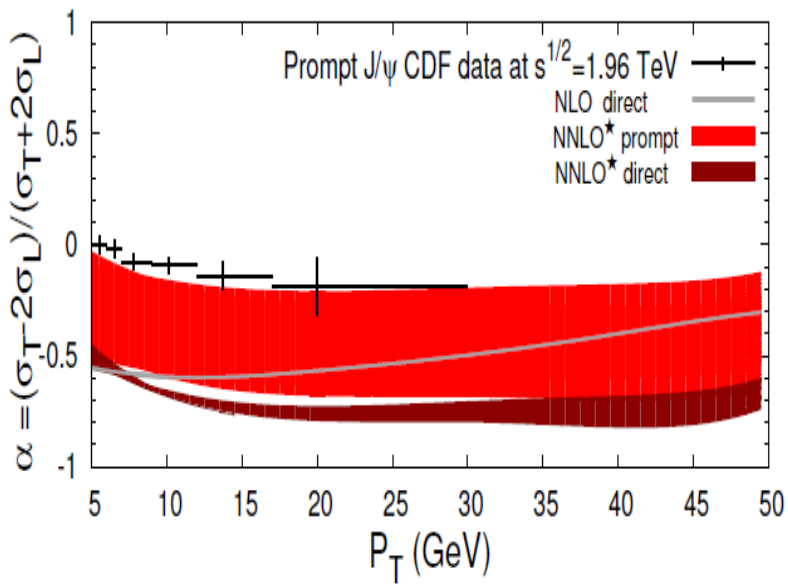

J.P.Lansberg (2011)

Fit CO LDMEs by including polarization

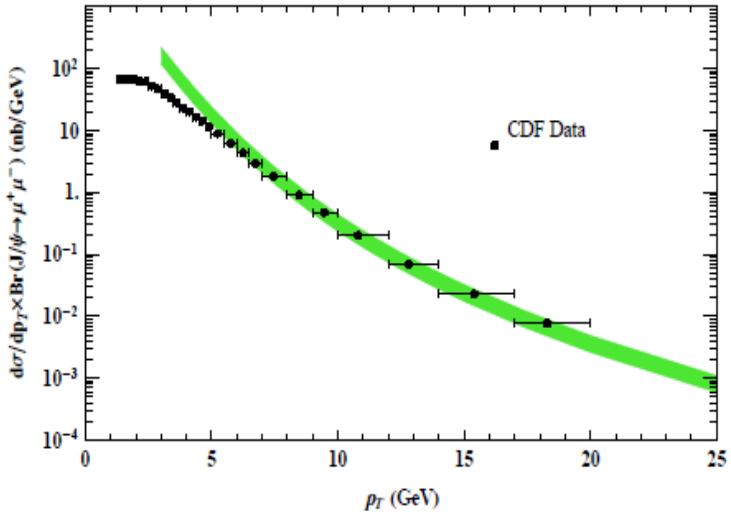

KTC, et al. (2012)

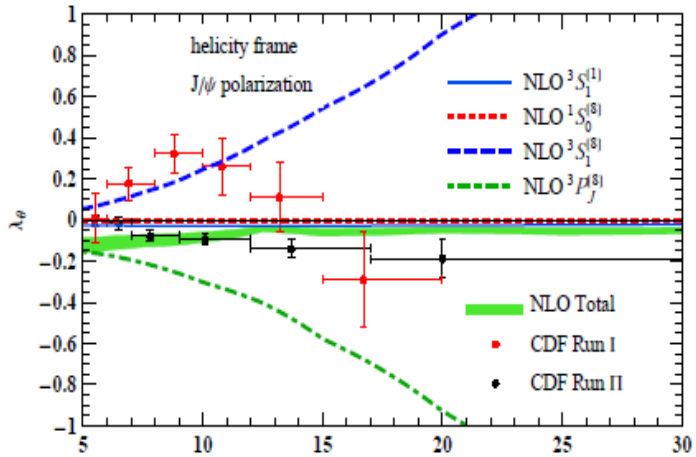

$$M_{0,r_0} = \langle \mathcal{O}(^1S_0^{[8]}) \rangle + \frac{r_0}{m_c^2} \langle \mathcal{O}(^3P_0^{[8]}) \rangle$$

$$M_{1,r_1} = \langle \mathcal{O}(^3S_1^{[8]}) \rangle + \frac{r_1}{m_c^2} \langle \mathcal{O}(^3P_0^{[8]}) \rangle$$

[Y.Q.Ma & K.Wang & K.T.Chao (2011)]

$\langle \mathcal{O}(^3S_1^{[1]}) \rangle$ GeV^3	M_{0,r_0} 10^{-2}GeV^3	M_{1,r_1} 10^{-2}GeV^3
1.16	7.4 ± 1.9	0.05 ± 0.02

$\Downarrow$ χ^2 fit to $\frac{d\sigma}{dp_T}$ and λ_θ

Compatible !

$\langle \mathcal{O}(^3S_1^{[1]}) \rangle$ GeV^3	$\langle \mathcal{O}(^1S_0^{[8]}) \rangle$ 10^{-2}GeV^3	$\langle \mathcal{O}(^3S_1^{[8]}) \rangle$ 10^{-2}GeV^3	$\langle \mathcal{O}(^3P_0^{[8]}) \rangle / m_c^2$ 10^{-2}GeV^3
1.16	8.9 ± 0.98	0.30 ± 0.12	0.56 ± 0.21
1.16	0	1.4	2.4
1.16	11	0	0

Prediction @ LHC

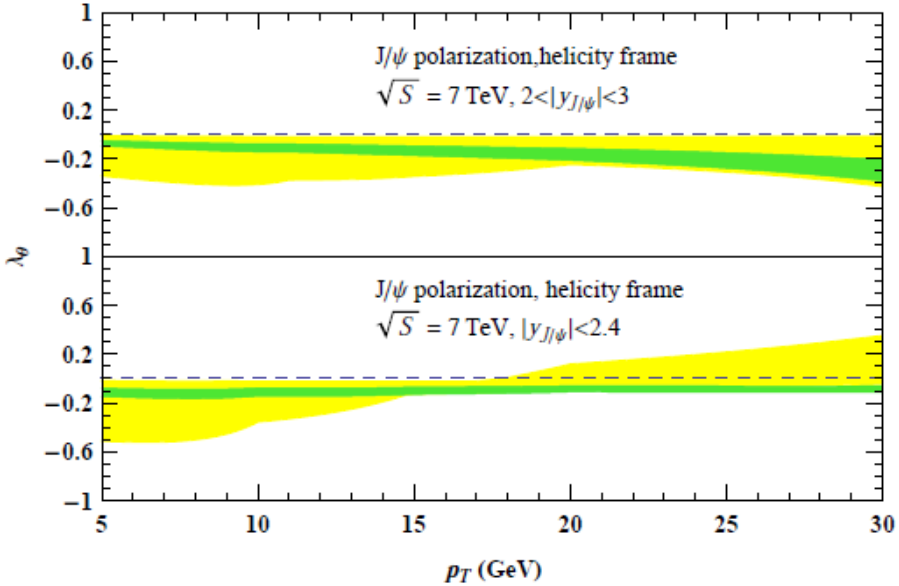

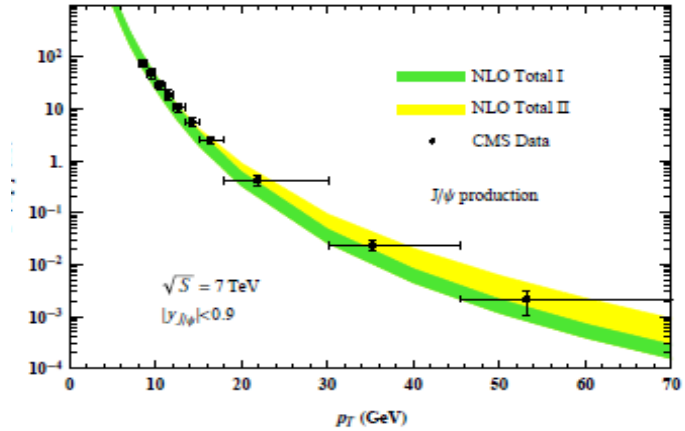

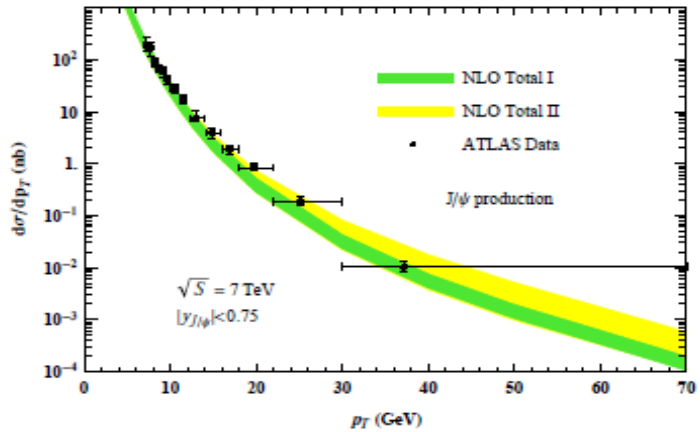

KTC, et al. (2012)

- Good for the pT distribution of cross section up to 70 GeV at the LHC.
- To predict un-polarized results at hadron colliders, a linear combination of CO LDMEs similar to M1 should be near zero.
- Lack of feed-down contributions.

χc polarization I

KTC, et al. (in preparation)

- J/ψ polar angular distribution in $\chi_c \to J/\psi\gamma$:

$$\frac{d\mathcal{N}^{\chi_{cJ}}}{d\cos\theta} \propto 1 + \sum_{k=1}^{J} \lambda_{k\theta} \cos^{2k}\theta,$$

- For χ_{c1} :

$$\lambda_\theta = (1-3\delta)\frac{N_{\chi_{c1}} - 3\rho_{0,0}^{\chi_{c1}}}{(1+\delta)N_{\chi_{c1}} + (1-3\delta)\rho_{0,0}^{\chi_{c1}}}$$

- For χ_{c2} :

$$\begin{aligned}\lambda_\theta &= 6[(1-3\delta_0-\delta_1)N_{\chi_{c2}} \\ &- (1-7\delta_0+\delta_1)(\rho_{1,1}^{\chi_{c2}} + \rho_{-1,-1}^{\chi_{c2}}) \\ &- (3-\delta_0-7\delta_1)\rho_{0,0}^{\chi_{c2}}]/R, \\ \lambda_{2\theta} &= (1+5\delta_0-5\delta_1)[N_{\chi_{c2}} - 5(\rho_{1,1}^{\chi_{c2}} + \rho_{-1,-1}^{\chi_{c2}}) \\ &+ 5\rho_{0,0}^{\chi_{c2}}]/R,\end{aligned}$$

$$\begin{aligned}R &= (1+5\delta_0+3\delta_1)N_{\chi_{c2}} \\ &+ 3(1-3\delta_0-\delta_1)(\rho_{1,1}^{\chi_{c2}} + \rho_{-1,-1}^{\chi_{c2}}) \\ &+ (5-7\delta_0-9\delta_1)\rho_{0,0}^{\chi_{c2}}.\end{aligned}$$

- Where:

$$\begin{aligned}\delta &= (1+2a_1^{J=1}a_2^{J=1})/2, \\ \delta_0 &= [1+2a_1^{J=2}(\sqrt{5}a_2^{J=2}+2a_3^{J=2}) \\ &+ 4a_2^{J=2}(a_2^{J=2}+\sqrt{5}a_3^{J=2}) + 3(a_3^{J=2})^2]/10, \\ \delta_1 &= [9+6a_1^{J=2}(\sqrt{5}a_2^{J=2}-4a_3^{J=2}) \\ &- 4a_2^{J=2}(a_2^{J=2}+2\sqrt{5}a_3^{J=2}) + 7(a_3^{J=2})^2]/30.\end{aligned}$$

Including multipole amplitudes, siginificant !

χc polarization II

KTC, et al. (in preparation)

- Di-lepton polar angular distribution in $\chi_c \to J/\psi\gamma \to l^+l^-\gamma$ with Z'=v2 :

$$\frac{d\mathcal{N}^{\chi_{cJ}}}{d\cos\theta'} \propto 1 + \lambda_{\theta'}\cos^2\theta',$$

- For χ_{c1} :

$$\lambda_{\theta'}^{\chi_{c1}} = \frac{-N_{\chi_{c1}} + 3\rho_{0,0}^{\chi_{c1}}}{R_1},$$

- For χ_{c2} :

$$\lambda_{\theta'}^{\chi_{c2}} = \frac{6N_{\chi_{c2}} - 9(\rho_{1,1}^{\chi_{c2}} + \rho_{-1,-1}^{\chi_{c2}}) - 12\rho_{0,0}^{\chi_{c2}}}{R_2},$$

- Where:

$$\begin{aligned}
R_1 &= [(15 - 2(a_2^{J=1})^2)N_{\chi_{c1}} \\
&- (5 - 6(a_2^{J=1})^2)\rho_{0,0}^{\chi_{c1}}]/(5 - 6(a_2^{J=1})^2), \\
R_2 &= [2(21 + 14(a_2^{J=2})^2 + 5(a_3^{J=2})^2)N_{\chi_{c2}} \\
&+ 3(7 - 14(a_2^{J=2})^2 - 5(a_3^{J=2})^2)(\rho_{1,1}^{\chi_{c2}} + \rho_{-1,-1}^{\chi_{c2}}) \\
&+ 4(7 - 14(a_2^{J=2})^2 - 5(a_3^{J=2})^2)\rho_{0,0}^{\chi_{c2}}] \\
&/ (7 - 14(a_2^{J=2})^2 - 5(a_3^{J=2})^2).
\end{aligned}$$

Including multipole amplitudes, negligible !

Normalized multipole amplitudes

Experiment	$a_2^{J=1}(10^{-2})$
CLEO[26]	$-6.26 \pm 0.63 \pm 0.24$
Crystal Ball [27]	$-0.2^{+0.8}_{-2.0}$
E835 [29]	$0.2 \pm 3.2 \pm 0.4$

Experiment	$a_2^{J=2}(10^{-2})$	$a_3^{J=2}(10^{-2})$
CLEO(Fit 1)[26]	$-9.3 \pm 1.6 \pm 0.3$	0(fixed)
CLEO(Fit 2)[26]	$-7.9 \pm 1.9 \pm 0.3$	$1.7 \pm 1.4 \pm 0.3$
Crystal Ball [27]	$-33.3^{+11.6}_{-29.2}$	0(fixed)
E760(Fit 1) [28]	-14 ± 6	0(fixed)
E760(Fit 2) [28]	-14^{+8}_{-7}	0^{+6}_{-5}
E835(Fit 1) [29]	$-9.3^{+3.9}_{-4.1} \pm 0.6$	0(fixed)
E835(Fit 2) [29]	$-7.6^{+5.4}_{-5.0} \pm 0.9$	$2.0^{+5.5}_{-4.4} \pm 0.9$

Our choice !

Single quark radiation

χc polarization @ LHC

KTC, et al. (in preparation)

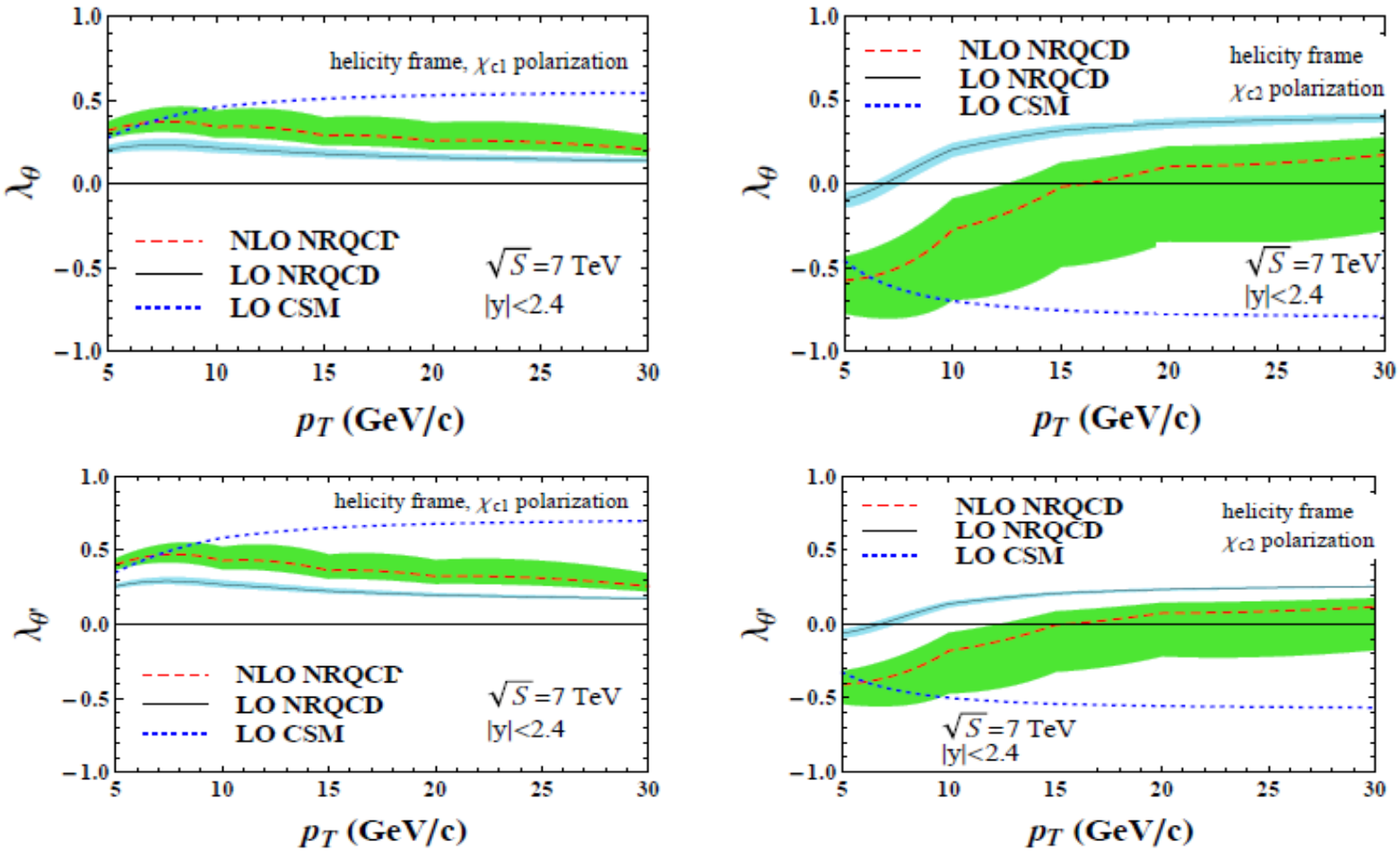

Summary

- Based on NRQCD factorization, we study both the yields and polarizations of heavy quarkonium production at the Tevatron and LHC at NLO including both CS and CO.

- The perturbative series are expected to be stable beyond NLO .

- Based on our NLO results, we make an effort to extract the three independent CO LDMEs by including the yields and polarization data at the Tevatron. However, the data are still insufficient to constrain these LDMEs stringently. Nevertheless, the two combinations of LDMEs can describe well the unpolarized J/ψ results both at the Tevatron and LHC.

- The predicted yields of J/ψ agree with the LHC data in our case up to 70 GeV. At high-pT region, can resummation of large logs change the fixed-order result much? We are interested in seeing it (see, Fleming, Leibovich, Mehen, Rothstein, arXiv:1207.2578)

- X_c provide another important test for CO mechanism in NRQCD. The yields and polarizations are all predicted here.

Summary

Long distance matrix elements extracted from hadron colliders are not compatible with that extracted from e+e- annihilation data by Belle for e+e-→J/psi+light hadrons, where CO contributions (1S0, 3PJ) should be very small , but CO 3S1 is not constrained (see Ma,Zhang,Chao, Phys.Rev.Lett.102:162002,2009 , Zhang,Ma,Wang,Chao, Phys.Rev.D81:034015,2010)

However, if CO 3S1 dominates, the polarization puzzle will remain, because CO 3S1 still leads to transverse polarization at NLO. Big difference between Belle and BaBar data exists? pQCD is not applicable for Belle data due to too low energy? Universality of LDMEs? Further investigations in both theory and experiment are needed!

Back up

Lagrangian for NRQCD

G.T.Bodwin et al. (1995)

$$\mathcal{L}_{\rm NRQCD} = \mathcal{L}_{\rm light} + \mathcal{L}_{\rm heavy} + \delta\mathcal{L}.$$

$$\mathcal{L}_{\rm light} = -\frac{1}{2}{\rm tr}\, G_{\mu\nu}G^{\mu\nu} + \sum \bar{q}\, i\not{D} q,$$

$$\mathcal{L}_{\rm heavy} = \psi^\dagger\left(iD_t + \frac{\mathbf{D}^2}{2M}\right)\psi + \chi^\dagger\left(iD_t - \frac{\mathbf{D}^2}{2M}\right)\chi,$$

$$\begin{aligned}
\delta\mathcal{L}_{\rm bilinear} = & \frac{c_1}{8M^3}\left(\psi^\dagger(\mathbf{D}^2)^2\psi - \chi^\dagger(\mathbf{D}^2)^2\chi\right) \\
& + \frac{c_2}{8M^2}\left(\psi^\dagger(\mathbf{D}\cdot g\mathbf{E} - g\mathbf{E}\cdot\mathbf{D})\psi + \chi^\dagger(\mathbf{D}\cdot g\mathbf{E} - g\mathbf{E}\cdot\mathbf{D})\chi\right) \\
& + \frac{c_3}{8M^2}\left(\psi^\dagger(i\mathbf{D}\times g\mathbf{E} - g\mathbf{E}\times i\mathbf{D})\cdot\boldsymbol{\sigma}\psi + \chi^\dagger(i\mathbf{D}\times g\mathbf{E} - g\mathbf{E}\times i\mathbf{D})\cdot\boldsymbol{\sigma}\chi\right) \\
& + \frac{c_4}{2M}\left(\psi^\dagger(g\mathbf{B}\cdot\boldsymbol{\sigma})\psi - \chi^\dagger(g\mathbf{B}\cdot\boldsymbol{\sigma})\chi\right),
\end{aligned}$$

$$\delta\mathcal{L}_{4-\rm fermion} = \sum_n \frac{f_n(\Lambda)}{M^{d_n-4}}\mathcal{O}_n(\Lambda),$$

e.g.

$$(\delta\mathcal{L}_{4-\rm fermion})_{d=6} = \frac{f_1(^1S_0)}{M^2}\mathcal{O}_1(^1S_0) + \frac{f_1(^3S_1)}{M^2}\mathcal{O}_1(^3S_1) + \frac{f_8(^1S_0)}{M^2}\mathcal{O}_8(^1S_0) + \frac{f_8(^3S_1)}{M^2}\mathcal{O}_8(^3S_1),$$

$$\mathcal{O}_1(^1S_0) = \psi^\dagger\chi\,\chi^\dagger\psi,$$

$$\mathcal{O}_1(^3S_1) = \psi^\dagger\boldsymbol{\sigma}\chi\cdot\chi^\dagger\boldsymbol{\sigma}\psi,$$

$$\mathcal{O}_8(^1S_0) = \psi^\dagger T^a\chi\,\chi^\dagger T^a\psi,$$

$$\mathcal{O}_8(^3S_1) = \psi^\dagger\boldsymbol{\sigma}T^a\chi\cdot\chi^\dagger\boldsymbol{\sigma}T^a\psi.$$

Power counting

G.T.Bodwin et al. (1995)

Operator	Estimate	Description
α_s	v	effective quark-gluon coupling constant
ψ	$(Mv)^{3/2}$	heavy-quark (annihilation) field
χ	$(Mv)^{3/2}$	heavy-antiquark (creation) field
D_t (acting on ψ or χ)	Mv^2	gauge-covariant time derivative
$\mathbf{D}$ (acting on ψ or χ)	Mv	gauge-covariant spatial derivative
$g\mathbf{E}$	M^2v^3	chromoelectric field
$g\mathbf{B}$	M^2v^4	chromomagnetic field
$g\phi$ (in Coulomb gauge)	Mv^2	scalar potential
$g\mathbf{A}$ (in Coulomb gauge)	Mv^3	vector potential

NRQCD Factorization

$$d\sigma_{\psi} = \sum_{i,j,n} \int \underbrace{dx_1 dx_2 \boxed{G_{i/A} G_{j/B}}}_{\Lambda_{QCD}} \times \underbrace{\boxed{\hat{\sigma}[ij \to c\bar{c}[n] + X]}}_{m_c} \times \underbrace{\boxed{\langle \mathcal{O}_n^{\psi} \rangle}}_{m_c v}$$

PDF

CTEQ6L1, CTEQ6M

Hadronization

Long distance (~1/(m_cv)) process: non-perturbative calculations and input from experiments needed.

Production of heavy quarks

Short distance (~1/m_c) process: perturbative calculation.

Main task in this work.

Code and packages

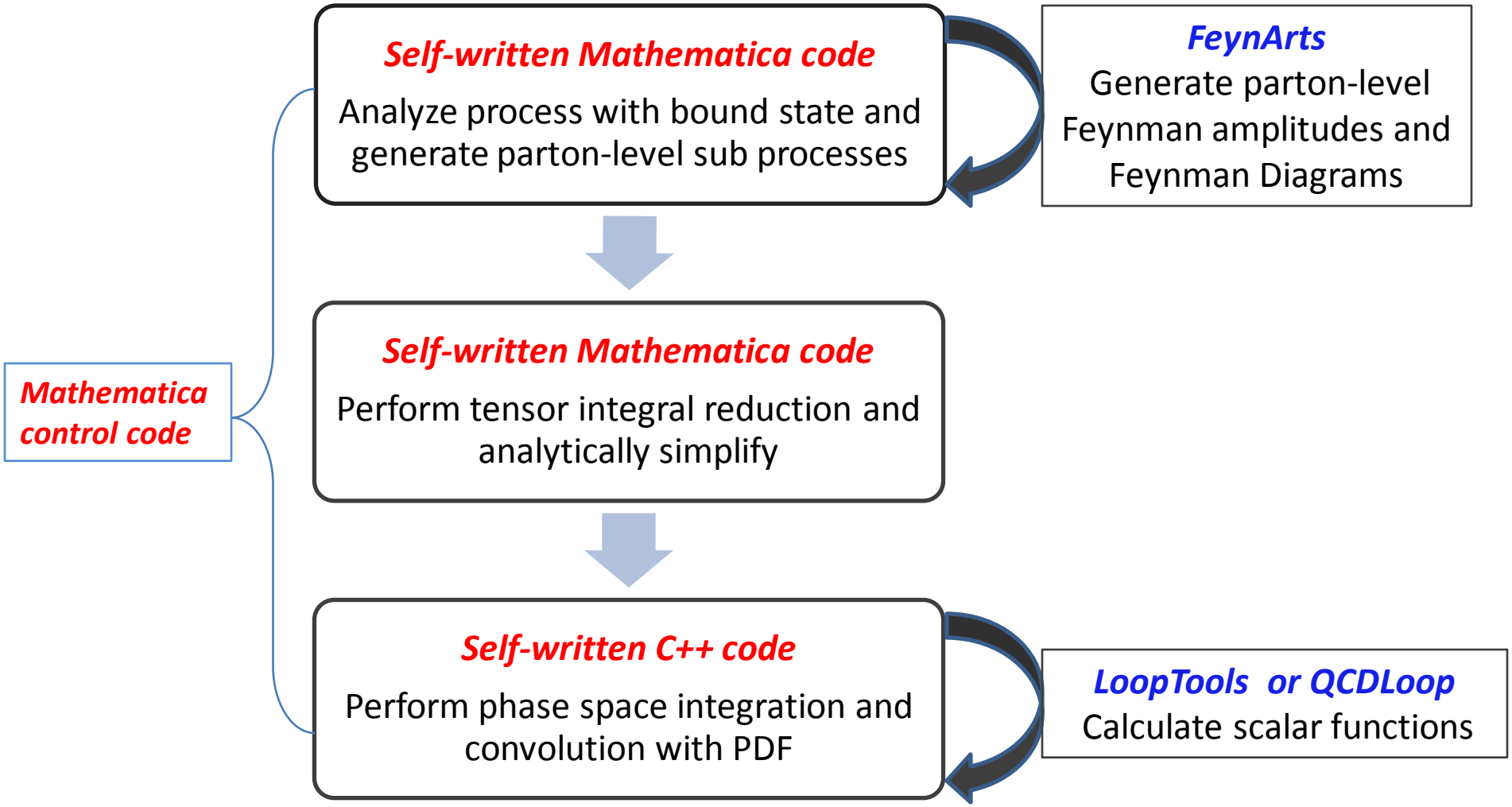

HELAC-ONIA

H.S.Shao, KTC (in preparation)

- ⋆ HELAC[2] generates the QCD and EW amplitudes at the partonic level based on Dyson-Schwinger equations.
- ⋆ PHEGAS[3] generates partonic level events with multi-channel techniques.
- ⋆ ONIA[4] generates hadronic (or quarkonium) level helicity amplitudes and physical observables based on the factorization of non-relativistic quantum chromodynamics[5].

---

[2] Note,refer to [*A.Kanaki & C.G.Papadopoulos (2000)*] and [*C.G.Papadopoulos & M.Worek (2006)*]

[3] Note,refer to [*C.G.Papadopoulos (2000)*].

[4] To be published in the future.

[5] Note,refer to [*G.T.Bodwin & E. Braaten & G.P.Lepage (1995)*].

Feynman diagrams for J/Ψ production

For J/Ψ, as an example:

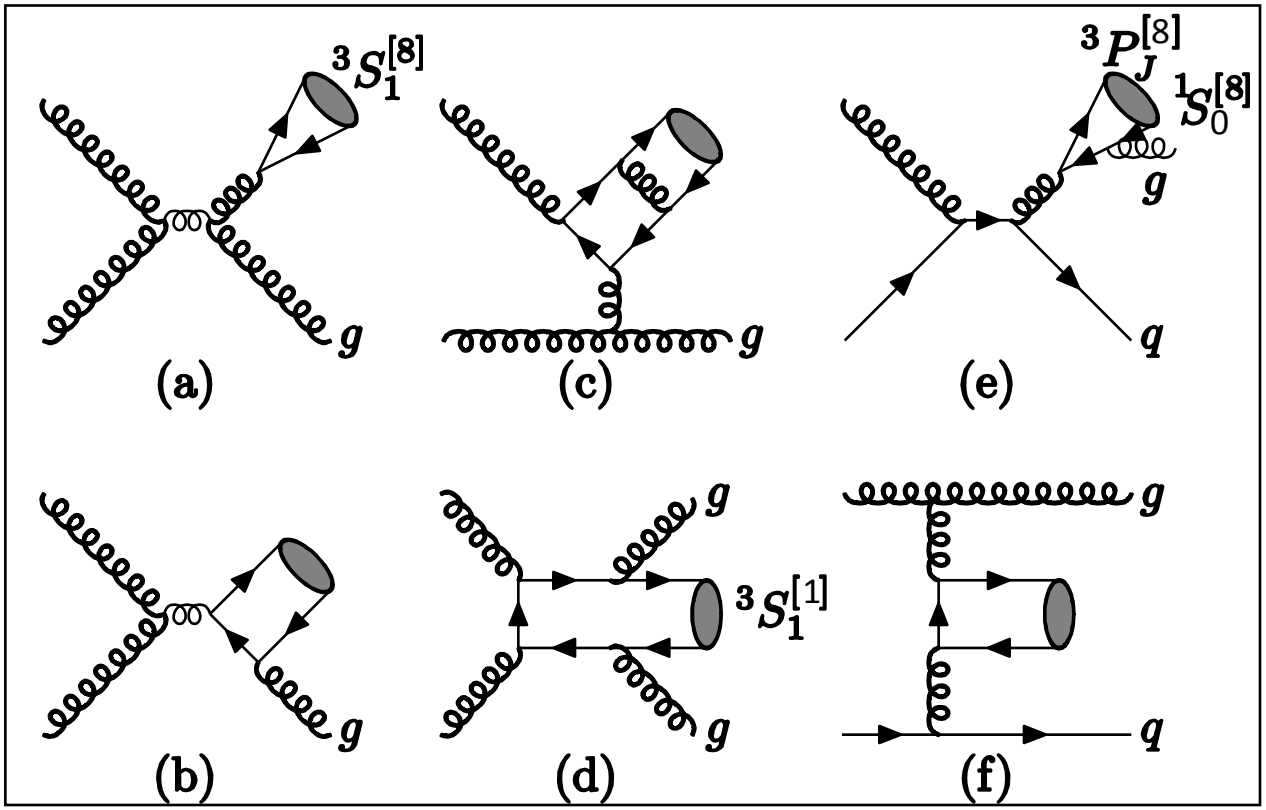

IR singularities

- Collinear singularities:

Independent of Heavy Quarkonium, cancel as jet production.

- Soft Singularities of S-wave channels:

Real + Virtual

- Soft Singularities of P-wave channels:

NRQCD MEs + Real + Virtual

$$\boxed{\mathcal{M}^{\mathrm{R}}\,|_s = g\,\mu_r^{\epsilon}\,\varepsilon_\mu J_f^{a,\mu}\,\mathcal{M}_f^{Born}}$$

$$\boxed{\mathcal{M}^{V}\,|_s = \frac{1}{2} g^2 \mu_r^{2\epsilon} I_{ff'}\,\mathcal{M}_{ff'}^{Born}}$$

where $J_f^{a,\mu} = \dfrac{p_f^{\mu}}{p_f \cdot k} T_f^a$ and $I_{ff'} = J_f^{a,\mu} J_{f',\mu}^{a}$

While $\mathcal{M}_f^{Born}$ and $\mathcal{M}_{ff'}^{Born}$ are color connected born level amplitudes.

Divergence cancelation

It can be shown that,

$$\left(T_f^a T_{f'}^a \mathcal{M}_{ff'}^{Born}\right)^\dagger \left(M^{Born}\right) = \left(T_f^a \mathcal{M}_f^{Born}\right)^\dagger \left(T_{f'}^a \mathcal{M}_{f'}^{Born}\right),$$

$$\left(T_f^a T_{f'}^a \mathcal{M}_{ff'}^{Born}\right)\left(M^{Born}\right)^\dagger = \left(T_f^a \mathcal{M}_f^{Born}\right)\left(T_{f'}^a \mathcal{M}_{f'}^{Born}\right)^\dagger, \; f' \neq Q, \overline{Q}$$

So only term that is not canceled between Real and Virtual is the P-wave term:

$$\boxed{-g^2 \mu_r^{2\epsilon} \varepsilon^\alpha \varepsilon^\beta \frac{\partial J_F^{a,\mu}}{\partial q^\alpha} \frac{\partial J_{F',\mu}^a}{\partial q^\beta} \left|\mathcal{M}^{Born}\right|^2_{FF'}}$$

Where $F, F' = Q \; or \; \bar{Q}$ and q is the relative momentum of heavy quarks.
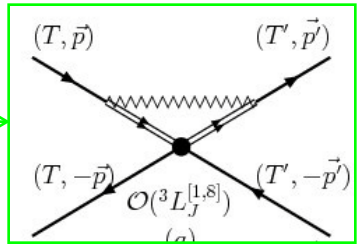
Finally, the above divergence can be absorbed by NRQCD MEs: